JOURNAL OF GEOPHYSICAL RESEARCH: ATMOSPHERES, VOL. 118, 8067–8085, doi:10.1002/jgrd.50537, 2013

Nitrogen, Aerosol Composition, and Halogens on a Tall Tower (NACHTT): Overview of a wintertime air chemistry field study in the front range urban corridor of Colorado

Steven S. Brown,[1] Joel A. Thornton,[2] William C. Keene,[3] Alexander A. P. Pszenny,[4] Barkley C. Sive,[4,5] William P. Dubé,[1,6] Nicholas L. Wagner,[1,6] Cora J. Young,[1,6,7] Theran P. Riedel,[2] James M. Roberts,[1] Trevor C. VandenBoer,[7,8] Roya Bahreini,[1,6,9] Fatma Öztürk,[1,10] Ann M. Middlebrook,[1] Saewung Kim,[11,12] Gerhard Hübler,[1,6] and Daniel E. Wolfe[1]

Received 8 March 2013; revised 28 May 2013; accepted 29 May 2013; published 30 July 2013.

[1] The Nitrogen, Aerosol Composition, and Halogens on a Tall Tower (NACHTT) field experiment took place during late winter, 2011, at a site 33 km north of Denver, Colorado. The study included fixed-height measurements of aerosols, soluble trace gases, and volatile organic compounds near surface level, as well as vertically resolved measurements of nitrogen oxides, aerosol composition, soluble gas-phase acids, and halogen species from 3 to 270 m above ground level. There were 1928 individual profiles during the three-week campaign to characterize trace gas and aerosol distributions in the lower levels of the boundary layer. Nitrate and ammonium dominated the ionic composition of aerosols and originated primarily from local or regional sources. Sulfate and organic matter were also significant and were associated primarily with longer-range transport to the region. Aerosol chloride was associated primarily with supermicron size fractions and was always present in excess of gas-phase chlorine compounds. The nighttime radical reservoirs, nitryl chloride, $ClNO_2$, and nitrous acid, HONO, were both consistently present in nighttime urban air. Nitryl chloride was especially pronounced in plumes from large point sources sampled aloft at night. Nitrous acid was typically most concentrated near the ground surface and was the dominant contributor (80%) to diurnally averaged primary OH radical production in near-surface air. Large observed mixing ratios of light alkanes, both in near-surface air and aloft, were attributable to local emissions from oil and gas activities.

Citation: Brown, S. S., et al. (2013), Nitrogen, Aerosol Composition, and Halogens on a Tall Tower (NACHTT): Overview of a wintertime air chemistry field study in the front range urban corridor of Colorado, *J. Geophys. Res. Atmos.*, *118*, 8067–8085, doi:10.1002/jgrd.50537.

1. Introduction

[2] The Nitrogen, Aerosol Composition, and Halogens on a Tall Tower (NACHTT) campaign took place during winter (17 February – 14 March) 2011 at the Boulder Atmospheric Observatory (BAO), located 33 km north of Denver, CO and within the urban/suburban corridor of Colorado's front range cities (Figure 1). The campaign addressed current uncertainties in oxidant and aerosol formation, as well as

[1]Chemical Sciences Division, Earth System Research Laboratory, NOAA, Boulder, Colorado, USA.
[2]Department of Atmospheric Sciences, University of Washington, Seattle, Washington, USA.
[3]Department of Environmental Sciences, University of Virginia, Charlottesville, Virginia, USA.
[4]Institute for the Study of Earth Oceans and Space, University of New Hampshire, Durham, New Hampshire, USA.
[5]Department of Chemistry, Appalachian State University, Boone, North Carolina, USA.
[6]Cooperative Institute for Research in Environmental Sciences, University of Colorado, Boulder, Colorado, USA.
[7]Department of Chemistry, Memorial University, St. Johns, Newfoundland, Canada.
[8]Department of Chemistry, University of Toronto, Toronto, Ontario, Canada.
[9]Department of Environmental Sciences, University of California, Riverside, California, USA.
[10]Environmental Engineering Department, Faculty of Engineering and Architecture, Abant Izzet Baysal University, Bolu, Turkey.
[11]Atmospheric Chemistry Division, Earth System Laboratory, National Center for Atmospheric Research, Boulder, Colorado, USA.
[12]Department of Earth System Science, School of Physical Sciences, University of California, Irvine, California, USA.

Corresponding author: S. S. Brown, Chemical Sciences Division, Earth System Research Laboratory, NOAA, Boulder, CO 80305, USA. (steven.s.brown@noaa.gov)

2169-897X/13/10.1002/jgrd.50537

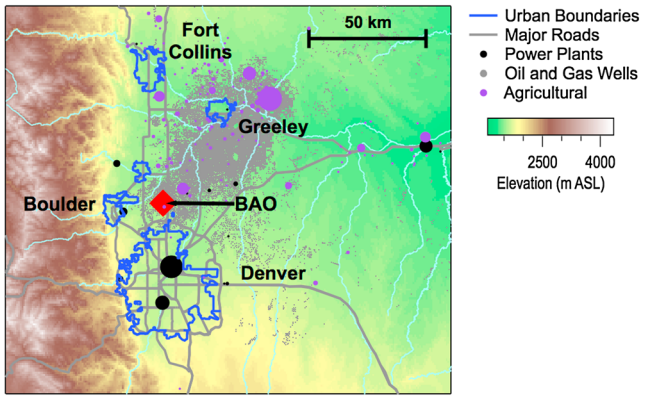

Figure 1. Map of the Front Range urban corridor of Colorado, showing major urban areas and roads, power plants (scaled by their relative NO_x emissions in 2006), oil and gas wells, and large agricultural facilities (scaled by the relative number of animals). The red diamond marks the location of the Boulder Atmospheric Observatory (BAO).

the interactions between oxidants and aerosols through heterogeneous chemical processes. The study also provided data on emissions and atmospheric chemistry relevant to current air quality issues in Colorado, including urban and power plant emissions, agricultural emissions, nitrate aerosol formation associated with winter haze in Denver, and emissions from oil and gas development in the Denver-Julesburg basin to the north of the urban area (Figure 1). The NACHTT campaign is a unique data set for understanding wintertime atmospheric chemistry and its coupling to boundary layer dynamics since it took place in an area influenced by this complex mix of emissions and included instrumentation and vertically resolved measurements able to characterize the chemical transformations that occur during cold, dark periods.

[3] Many previous field investigations of emissions and chemical transformation relevant to air quality concerns have taken place during summer months and/or warm conditions when higher rates of photochemistry and higher temperatures lead to rapid production of secondary ozone and organic aerosol (OA). Although a number of important issues are specific to polluted wintertime environments, detailed wintertime intensive field studies are less common. Accumulation of aerosol mass in excess of National Ambient Air Quality Standards (NAAQS, currently 35 $\mu g\,m^{-3}$ for PM 2.5, particulate matter (PM) less than 2.5 μm diameter, 24 h average), particularly ammonium nitrate aerosols, tends to be a winter phenomenon due to the temperature-dependent phase partitioning of nitric acid and ammonia [*Chen et al.*, 2010; *Chen et al.*, 2012; *Fischer and Talbot*, 2005; *Katzman et al.*, 2010; *Mathur et al.*, 2008; *Schaap et al.*, 2004; *Stanier et al.*, 2012; *Tolocka et al.*, 2001; *Yu et al.*, 2005]. Air quality models often fail to accurately predict nitrate aerosol, due to the complexity of both the chemistry and the shallow boundary layers typically associated with these episodes. In addition, recent observations in the western United States show that photochemical ozone production can be a severe air quality issue during wintertime in polluted mountain basins that are impacted by emissions of volatile organic compounds (VOCs) and nitrogen oxides ($NO_x = NO + NO_2$) from oil and gas exploration [*Carter and Seinfeld*, 2012; *Schnell et al.*, 2009]. Here again, cold pool meteorology and concentration of pollutants within shallow boundary layers play an important role [*Baker et al.*, 2011]. Finally, oxidation pathways are important in the chemical evolution of all primary emissions during winter, but they are normally much slower than in summer, and can be dominated by sources other than ozone photolysis, the major global source of primary OH [*Levy*, 1971]. Measured radical levels during winter have far exceeded model predictions in several instances, suggesting a lack of understanding of winter oxidant formation processes [*Cai et al.*, 2008; *Fleming et al.*, 2006; *Heard et al.*, 2004; *Ren et al.*, 2006]. Accurate understanding of radical and oxidant sources is required to reliably predict the chemical processing, transport, lifetime, and environmental consequence of short-lived primary and secondary pollutants.

[4] Recent field and laboratory work has identified two key oxidant sources related to the heterogeneous chemistry of nitrogen oxides that are likely prevalent in winter. Conversion of NO_x to soluble nitrate through heterogeneous uptake of N_2O_5, a predominantly nighttime species, has long been understood as the major loss process for nitrogen oxides in winter, with consequences for global tropospheric ozone budgets [*Dentener and Crutzen*, 1993] and regional formation of nitrate aerosol [*Riemer et al.*, 2003]. Production of nitryl chloride, $ClNO_2$, from reaction of N_2O_5 with particulate chloride (Cl^-) was first demonstrated in the laboratory by Finlayson-Pitts *et al.* [*Finlayson-Pitts et al.*, 1989], but was only recently verified in the atmosphere from ambient measurements [*Osthoff et al.*, 2008].

$$N_2O_5(g) + Cl^-(aq) \rightarrow ClNO_2(g) + NO_3^-(aq) \qquad (R1)$$

[5] Recent field investigations have shown that $ClNO_2$ production from N_2O_5 uptake in the nighttime atmosphere is efficient [*Kercher et al.*, 2009; *Mielke et al.*, 2011; *Osthoff et al.*, 2008; *Phillips et al.*, 2012; *Riedel et al.*, 2012a; *Thornton et al.*, 2010; *Wagner et al.*, 2012]. Photolysis of $ClNO_2$ following sunrise produces atomic chlorine, a powerful oxidant, and recycles NO_2. A 2009 study investigated $ClNO_2$ production at the Kohler mesa site just west of Boulder, CO, a location well removed from large sources of aerosol Cl^- from sea spray [*Thornton et al.*, 2010]. This study, along with an analysis of the distribution of particulate Cl^- from long-term monitoring network data, demonstrated that halogen activation *via* this chemistry is ubiquitous, occurring with appreciable yields even in interior continental regions. A large fraction of the inferred halogen activation occurs during winter months, when nighttime N_2O_5 chemistry is most prevalent. Key uncertainties identified in this study that limited complete understanding of $ClNO_2$ formation included the distribution of nitrogen oxides within the stratified nighttime boundary layer, the sources of and reservoirs for particulate Cl^-, and the composition (including acidity) and hydration and mixing state of the aerosol on which N_2O_5 uptake occurs.

[6] Heterogeneous uptake of NO_2 to surfaces produces nitrous acid, HONO, also a nighttime radical reservoir species. The reaction may be written as a disproportionation, yielding both nitrous and nitric acids, shown here for simplicity as gas-phase products.

$$2NO_2(g) + H_2O(l) \rightarrow HNO_3(g) + HONO(g) \qquad (R2)$$

[7] Nitrous acid accumulates in the dark but photolyzes following sunrise to produce both OH radicals and NO. Although

HONO has been known from ambient measurements for several decades [*Perner and Platt*, 1979], the mechanism for the net reaction shown in (R2) remains controversial [*Finlayson-Pitts et al*., 2003]. Vertically resolved ambient HONO measurements typically show strong gradients near-surface level [*Kleffmann et al*., 2003; *Stutz et al*., 2002; *Stutz et al*., 2010; *Zhang et al*., 2009], suggesting that reaction (R2) occurs readily on ground surfaces but less readily via uptake to aerosol surfaces. This behavior is in contrast to that of $ClNO_2$, for which the limited available vertical data suggest it does not exhibit strong gradients, at least near coastal areas rich in sea salt aerosol [*Young et al*., 2012]. Ambient measurements of HONO during daytime suggest further that (1) rates of NO_2 conversion to HONO must be greater during daytime than at night (perhaps photochemically enhanced) and (2) HONO photolysis may provide a large source of OH radicals during daytime [*Stemmler et al*., 2006; *Su et al*., 2008].

[8] The context for NACHTT was the investigation of wintertime oxidant and aerosol formation in an area with complex emissions. The campaign addressed several interrelated scientific objectives. (1) To characterize the efficiency of wintertime halogen activation at a polluted, midcontinental site, including the efficiency of NO_x conversion to $ClNO_2$, and the mass balance for the cycling between HCl, $ClNO_2$, and particulate Cl^-. An important component of this objective was to characterize the vertical structure of NO_x within the nocturnal boundary layer and the efficiencies of heterogeneous processes as a function of height. (2) To obtain an improved inventory for gas and aerosol phase chloride, thought to be the limiting reagent for halogen activation. This objective included chemical correlations of gas and aerosol phase chloride with other species, size-resolved distributions of particulate Cl^-, and where possible, understanding of chloride emissions from different sources, and tracers for relative influence of long-range transport versus local sources. (3) An improved understanding of inorganic aerosol thermodynamics and its relationship to the heterogeneous processes discussed above. (4) Characterization of the wintertime uptake efficiency of N_2O_5 by aerosols, for which there is a growing database of summertime determinations [*Bertram et al*., 2009; *Brown et al*., 2006b; *Brown et al*., 2009; *Riedel et al*., 2012b], but fewer analyses based on ambient measurements in winter, when this process is relatively more important. (5) To develop an understanding of wintertime radical reservoirs and budgets through the comparison of vertically resolved radical production via $ClNO_2$ and HONO to that from O_3 photolysis. (6) To understand aerosol composition and sources that lead to formation of urban haze within the Denver area. Winter aerosol pollution is a long-standing problem within this airshed. Detailed composition measurements with vertical resolution can provide a unique perspective for evaluating this problem. (7) To characterize emissions from the oil and gas industry and their impact on local air quality. Speciated VOC measurements with vertical resolution, originally included in the study in order to ascertain the potential influence of chlorine radicals on oxidation, are also useful in quantifying emissions from the oil and gas sector.

2. Previous Air Quality Studies in Colorado's Front Range Urban Corridor

[9] Wintertime air pollution episodes within the Denver urban area and its surroundings, commonly referred to as the "Denver Brown Cloud," are well documented. As early as the 1960s, there were field intensives and modeling efforts to understand the local meteorology and the sources of aerosols and other pollutants associated with these events (see [*Riehl and Herkhof*, 1972] and references therein). These early studies reported average total mass loadings for PM of 150 $\mu g\,m^{-3}$, with maximum values in excess of 300 $\mu g\,m^{-3}$ associated with low wind and shallow boundary layer conditions within the city of Denver [*Riehl and Herkhof*, 1972]. The first major field intensive aimed at understanding the complete chemical characteristics of the Denver Brown Cloud took place during a two-week period in November 1973 under sponsorship of the U.S. Environmental Protection Agency [*Russell*, 1977]. This study included meteorological analysis that demonstrated diurnal flow reversal patterns, with a nighttime drainage flow to the northeast, along the South Platte River valley, with a characteristic change in flow direction during late morning or midday [*Crow*, 1977]. (Similar flow reversal patterns are also characteristic of summer months when particulate air pollution episodes are less severe [*Toth and Johnson*, 1985].) The 1973 study notably included aircraft measurements of major gas-phase (O_3, NO_x, CO, SO_2) and aerosol (size distribution) pollutants [*Anderson et al*., 1977]. The aircraft measurements demonstrated that the mixing height within the urban plume varied from 150 to 600 m during daytime and that emissions from buoyant point sources (power plants) formed layers aloft that were ventilated to surface level as the mixed layer deepened. Photochemistry was an important driver for changes in both ozone concentration (up to a maximum value 80 ppbv relative to a background of 30–50 ppbv) and PM size distributions during downwind evolution of the Denver urban plume. Analysis of data from the 1973 study also identified aerosol optical properties, rather than absorption due to NO_2, as the cause of the characteristic brown color of Denver wintertime haze [*Waggoner*, 1977].

[10] *Haagenson* [1979] examined meteorological factors that lead to trapping of pollutants within the Denver basin in wintertime from ten years of regular sounding data at Stapleton Airport in Denver together with detailed sounding data from a 1977 study. This analysis focused on the role of ventilation (i.e., wind speed) and mixing depth, as in other studies, as well as on the role of stability above the mixed layer, a factor peculiar to Denver due to downslope flow along the Rocky Mountains in winter. For example, an episode in December 1977 characterized by a low daytime mixing height (200 m) and high stability aloft ($\Delta T = +20°C$ from 200 to 600 m) led to accumulation of CO to a mixing ratio of 17 parts per million by volume (ppmv) within the city. Later meteorological methods have become more sophisticated and successful in their ability to predict wintertime haze events [*Reddy et al*., 1995].

[11] A field study in the Commerce City area on the northeast side of Denver in November – December 1978 included measurements of both gas-phase pollutants and aerosol composition. Fine-mode (<1 μm) aerosol had a large contribution from ammonium nitrate, in contrast to other U.S. cities, which were sulfate dominated at that time. Coarse-mode aerosol, by contrast, was found to be mostly (75%) soil-like material [*Countess et al*., 1980; *Countess et al*., 1981]. Photochemical production of both ozone and nitrate aerosol was important during winter days with low temperatures, although the maximum 1 h ozone level of 63 ppbv did not exceed the NAAQS

for ozone at that time (80 ppbv, 1 h) [*Ferman et al*., 1981]. Levels of CO (2.48 ppmv, average), NO_x (125 ppbv average), and hydrocarbons (3.15 ppmC, average) were all elevated, with CO exceeding the 8 h average standard of 9 ppmv on three occasions. The gas and aerosol phase components responsible for visibility reductions included elemental carbon (38% of the optical extinction), ammonium sulfate and nitrate (20% and 17%), organic compounds (13%), other particulates (7%), and absorption by gas-phase NO_2 (6%) [*Groblicki et al*., 1981]. Attribution of the fine particulate mass (FPM) and visual range reduction (VRR) to specific emission sources found that motor vehicles were responsible for 26 and 27% of FPM and VRR, respectively, coal combustion >20 and >25%, and wood burning 12 and 18% [*Wolff et al*., 1981].

[12] A three-week study that included measurements of coarse and fine-mode aerosol composition, aerosol optical properties, and major gas-phase pollutants took place in January 1982 at a site 10 km northeast of downtown Denver [*Lewis et al*., 1986]. Source attribution for this study was similar to the 1978 results, with motor vehicle emissions (42% of fine particle mass and 47% of light extinction, respectively) representing the single largest source of winter haze, followed by electric power generation (23 and 44%, respectively) and wood combustion (12 and 14%). Fine-mode aerosol composition was dominated by elemental (10%) and organic (34%) carbon, sulfate (10%), nitrate (11%), and ammonium (6%), while silicon, aluminum, and chloride dominated the coarse mode. Coarse-mode aerosol was apportioned as 83% soil and 11% "street salt."

[13] The 1987–1988 Denver Metro Brown Cloud Study was a more extensive field campaign that encompassed three months from 1 November 1987 to 31 January 1988 at several sites along the Platte River extending from downtown Denver toward the northeast [*Burns et al*., 1990]. As in the prior studies, one of the main goals was to characterize visibility reductions and attribute the responsible emission sources, and the study included measurements of light extinction [*Dietrich et al*., 1990], aerosol mass and composition, gas-phase pollutants, and meteorology. The study included source profiling characteristics for different types of dust aerosol [*Houck et al*., 1990] as well as motor vehicle emissions [*Watson et al*., 1990]. Source apportionment showed absorption by elemental carbon to be the largest contributor to visibility reduction at 30%, even though it was only 20% of fine particle mass. Scattering by organic carbon accounted for 20% of light extinction, while this species accounted for 34% of fine particle mass [*Richards et al*., 1990]. Agricultural emissions of ammonia from large cattle feed lots to the northeast of the Denver urban area were identified as an important factor in the formation of ammonium sulfate and nitrate aerosol on the basis of measurements under northeasterly flow and more stagnant conditions [*Sloane et al*., 1990; *Sloane et al*., 1991]. The study was unusual in that it included a fuel switching experiment at electric power plants, which alternated between coal and natural gas combustion during the study period in order to test the influence of sulfur emissions on regional visibility [*Neff and Watson*, 1990]. Unfortunately, the data were inconclusive due to different meteorological conditions during periods of natural gas versus coal use, and due to the potential influence of long-range transport on local sulfate loadings in Denver. For example, even though sulfur dioxide and nitrogen oxide emissions underwent estimated 70 and 10% reductions, respectively, during natural gas burning periods, sulfate and nitrate mass loadings actually increased during these times.

[14] A following modeling study, Brown Cloud II (BC II) [*Neff*, 1997], suggested that a much wider emissions domain was required to explain the observations, including sources distributed throughout the South Platte river valley from Denver well to the northeast. While strong emissions of NO_x are concentrated in urban Denver, strong ammonia sources are concentrated further down valley in Greeley, and sulfur sources from power plant emissions come from as far northeast as Fort Morgan (marked in Figure 1 as the power plant and agricultural facility at the eastern edge of the displayed domain). These sources are connected by nighttime downslope drainage along the South Platte valley and thermally driven upslope during daytime. The BC II modeling effort specifically highlighted the need for more detailed vertically resolved measurements of boundary layer structure (and presumably chemical composition).

[15] The Northern Front Range Air Quality Study (NFRAQ) was the largest of its kind and was aimed, like its predecessors, at understanding sources of wintertime aerosol [*Watson et al*., 1998] and characteristics of their optical properties [*Moosmuller et al*., 1998]. It included two winter measurement intensives, one in January – February 1996 (44 days) and one from December 1996 to February 1997 (60 days), and one summer intensive during July and August 1996 (45 days). The study included a much larger measurement network, with nine sites spanning the area from downtown Denver 90 km north to Fort Collins, 80 km northeast along the South Platte river valley and south to the southern edge of the urban area. Wintertime aerosol mass loadings from this study were considerably lower, with a maximum PM2.5 level of 50 $\mu g\,m^{-3}$ well downwind of Denver and typical urban levels of 10–12 $\mu g\,m^{-3}$. There were no episodes that exceeded the 24 h national ambient air quality standard for PM2.5 at that time (65 $\mu g\,m^{-3}$). Carbonaceous aerosol was higher in urban Denver than in downwind sites but did not contribute more than 50% of total mass in either location. By far the largest source of carbonaceous aerosol was motor vehicle emissions (75–85%), with wood combustion amounting to a moderate (4–8%) contribution. Carbon 14 analysis showed aerosol carbon to be 73–77% fossil in origin, consistent with these findings [*Klinedinst and Currie*, 1999]. Secondary ammonium nitrate and ammonium sulfate was a large contribution to total mass throughout the domain, and more than 50% north of the Denver urban area, with ammonium nitrate two to four times larger than ammonium sulfate. The area was determined to be ammonia rich, with aerosol sulfate balanced on an equivalent basis by ammonium and total ammonia (gas + particle) in excess of total nitrate (gas + particle). Nitrogen oxide emissions from motor vehicles were identified as an important contributing factor to ammonium nitrate aerosol. Interestingly, although an air quality alert program was implemented with the intent of reducing motor vehicle traffic on episode days, a study undertaken during the same time period as NFRAQS showed this program to have no effect on driving habits [*Blanken et al*., 2001].

[16] The Rocky Mountain Airborne Nitrogen and Sulfur Studies (ROMANS) characterized nitrate and sulfate deposition and their sources to sensitive areas within the Rocky Mountains [*Levin et al*., 2009]. Deposition has been previously identified as an important issue within the region

[*Nanus et al*., 2003]. Data from the first ROMANS study in 2006 at a site in Rocky Mountain National Park showed ammonium sulfate and nitrate to be dominant components of aerosol mass in spring, when mass loadings were lower (2.2 $\mu g\,m^{-3}$ avg.), with organic carbon dominant in summer, when mass loadings were higher (6.5 $\mu g\,m^{-3}$ avg.) [*Levin et al*., 2009]. This study also included distributed measurements at sites across the northeastern plains of Colorado to the east of the Rocky Mountains. The second ROMANS study in 2008 included yearlong measurements at three sites, Rocky Mountain National Park, Loveland at the western edge of the plains, and Brush on the northeastern plains. Gas-phase ammonia and particulate ammonium showed little seasonality, while both gas-phase nitric acid and particulate nitrate showed a distinct pattern, with nitric acid maximum in summer and particulate nitrate maximum in winter [*Benedict et al*., 2013].

[17] *Brodin et al.* [2010] reported the seasonal cycle of ozone at surface sites along an east-west transect from Boulder through the Rocky Mountains to the west to assess the variation in ozone with altitude. Summertime measurements showed a distinct diurnal cycle at all elevations, while wintertime measurements showed a diurnal cycle only at the lowest elevation sites, with little apparent diurnal cycle at 350 m and no diurnal cycle for sites 750 m or greater above the urban area. These results are consistent with the impact of wintertime urban emissions being confined to low altitudes.

[18] Finally, the recent Denver Aerosol Sources and Health study has provided a longer-term data set for aerosol mass loading and composition to identify associations with health impacts [*Dutton et al*., 2010], following earlier studies that had shown health impacts in the Denver area due to ozone in summer [*Koken et al*., 2003] and PM in winter [*Silkoff et al*., 2005]. *Dutton et al.* [2010] reported seasonal trends in aerosol composition and gas-phase hydrocarbons from 4.5 years of data collected in Denver beginning in 2002. Like other sites in the U.S., nitrate and sulfate aerosol had opposing seasonal trends, with sulfate larger in summer and nitrate largest in winter. Organic carbon showed maxima in both winter and summer, with minima in spring and fall, while elemental carbon showed only a winter maximum.

[19] The NACHTT data set augments these prior measurements of atmospheric gas and aerosol phase chemical composition in Colorado's Front Range Cities in several respects. First, it is the only detailed data set that includes vertically resolved measurements of key species, including nitrogen oxides and aerosol composition through the range characteristic of the nighttime boundary layer structure. The 300 m tower height is sufficient to capture the daytime boundary layer structure during severe wintertime inversion episodes. Second, it includes detailed multiphase measurements of halogen species and nighttime nitrogen oxides, including nitrous acid. These compounds represent important radical precursors and intermediates that have been little studied in winter (see discussion in introductory section). Together with those of OH radicals, these measurements provide new understanding of wintertime oxidation mechanisms. Finally, the NACHTT study provides an additional wintertime data set to the existing body of literature that spans nearly four decades of intensive measurements within the Front Range, from which trends in gas and aerosol phase composition may be inferred.

3. Components of NACHTT

[20] The BAO is located 33 km north of the city center of Denver and 23 km east of the city center of Boulder (Figure 1). The NACHTT campaign took place entirely at the BAO site and included three distinct components. The first involved vertically resolved measurements of gases and aerosols from a movable carriage on the outside of one face of the 300 m research tower. These were augmented by canister samples at lower time resolution filled at different heights accessed from an elevator internal to the tower. The second included measurements of soluble gas- and aerosol-phase species measured from a fixed platform mounted to the main tower at 22 m above ground level. The third component included measurement of gases and radiation sampled either from the top of a 9 m scaffolding tower adjacent to the main tower or at a fixed height closer to ground level.

3.1. Vertically Resolved Measurements From the BAO Tower

[21] The BAO [*Kaimal and Gaynor*, 1983] has a 300 m research tower that is a unique facility for atmospheric chemical sampling [*Vanvalin and Ganor*, 1987] and meteorological measurements [*Hahn*, 1981]. The three-legged tower has an external carriage on its west-southwest face that has a payload capacity in excess of 1 ton and that is capable of ascent/descent rates of approximately 0.5 $m\,s^{-1}$ to enable measurement of one 300 m profile in approximately 10 min. During NACHTT, vertical profiles were limited to 250 m for the majority of the measurements and 270 m during the final week of the campaign. (A previous set of more limited chemical measurements in 2004 generated vertical profiles over the entire 300 m tower height [*Brown et al*., 2007]). For NACHTT, a steel frame, aluminum-sided instrument enclosure measuring 3.04 m width × 1.83 m depth × 1.83 m height was mounted to the external carriage for vertical profiling. The enclosure weighed approximately 800 lbs. (360 kg) and allowed for a total instrument payload of roughly 2000 lbs. (900 kg). This enclosure, known as the Profiling Instrument Shelter with Amenities (PISA), is temperature controlled and has an electrical capacity of approximately 15 kW for operation of scientific instruments. It includes a server that collects and provides a data stream containing height and meteorological data to all instruments. Data from each instrument can be fed back to the server and viewed remotely from a second server connected via a wireless link on the ground. Each individual instrument can also be monitored and controlled remotely via this link. The link also allows for remote control of the carriage movement on the tower. To ensure safety of operations during NACHTT, the carriage movement was monitored and controlled by an operator at all times rather than being fully automated. Height above ground is measured by both a global positioning system unit associated with the carriage data server, and by a device that counted the teeth on the tower drive mechanism, attached to the carriage motor. The latter has considerably higher accuracy (better than 10 cm). The electric drive motor did not have emissions that influenced any of the chemical measurements during NACHTT. Instruments were integrated into the PISA at the NOAA laboratories in Boulder, CO, 22 km west of the BAO site. The PISA was subsequently towed to the BAO site where it was mounted on the tower fully loaded.

Table 1. Vertically Resolved Measurements on BAO Tower

Species/Parameter	Reference	Method	Sample Frequency	Detection Limit	Uncertainty
NO, NO_2, O_3	*Wagner et al*., [2011]	405 nm CRDS[a]	1 s	NO_2: 50 pptv NO, O_3: 100 pptv	NO_2 3% NO, O_3 5%
NO_3, N_2O_5	*Wagner et al*., [2011]	662 nm CRDS	1 s	NO_3: 1 pptv N_2O_5: 2 pptv	NO_3, 20% N_2O_5, 11%
$ClNO_2$, Cl_2, N_2O_5	*Kercher et al*., [2009]	I^- CIMS[b]	10 s	5 pptv	20%
Inorganic acids	*Roberts et al*., [2010]	NI-PT-CIMS[c]	10 s	HCl: 70 pptv HNCO: 20 pptv HCOOH: 20 pptv HONO: 4 pptv HNO_3: 27 pptv	15%
Sub-μm aerosol composition	*Bahreini et al*., [2009]	AMS[d]	10 s	SO_4^{-2}, NO_3^-: 9 ng m^{-3} NH_4^+: 5 ng m^{-3} Cl^-: 1 ng m^{-3} Organics: 7 ng m^{-3}	33–37%
Aerosol size distributions, 0.07–0.8 μm	*Brock et al*., [2011]	UHSAS[e]	1 s		Number +22/−19% Surface +36/−27% Volume +45/−31%
CO_2		Open path NDIR[f]	1 s	0.04 ppmv	
Meteorological data (temp, pres, rel humidity, wind speed, wind direction)			1 s		
Speciated VOCs	*Russo et al*., [2010]; *Sive et al*., [2005]; *Zhou et al*., [2008]	Canister samples, GC-MS[g] analysis	two to three times/day	<10 pptv	NMHC 1–8% Alkyl nitrates 3–8% Halocarbons 4–15%

[a]Cavity Ring-Down Spectroscopy.
[b]Chemical Ionization Mass Spectrometry.
[c]Negative Ion Proton Transfer CIMS.
[d]Aerosol Mass Spectrometer.
[e]Ultra High Sensitivity Aerosol Spectrometer.
[f]Nondispersive Infrared Spectroscopy.
[g]Gas Chromatography-Mass Spectrometry.

[22] Instruments mounted in the PISA during NACHTT included a cavity ring-down spectrometer (CRDS) to measure nitrogen oxides (NO, NO_2, NO_3, N_2O_5) and ozone [*Fuchs et al*., 2009; *Wagner et al*., 2011; *Washenfelder et al*., 2011], a chemical ionization mass spectrometer (CIMS) with I^- reagent ion to measure N_2O_5 and halogen species ($ClNO_2$, Cl_2) [*Kercher et al*., 2009], a negative ion proton transfer reaction CIMS with acetate reagent ion to measure organic and inorganic acids (principal focus on inorganic acids during NACHTT) [*Roberts et al*., 2010; *Veres et al*., 2008], an aerosol mass spectrometer (AMS) for measurement of submicron aerosol composition [*Bahreini et al*., 2008; *Bahreini et al*., 2009], a laser optical particle counter for measurement of size distributions between 0.07 and 0.8 μm, from which submicron aerosol surface and volume could be derived [*Brock et al*., 2011] and carbon dioxide (Table 1). The reader is referred to the cited literature for further details on the operational characteristics of the gas and aerosol phase instruments. Meteorological measurements, which were critical for understanding air mass characteristics as a function of height above ground level, included temperature, pressure, relative humidity, wind speed, and wind direction. Potential temperature, a measure of static stability, was derived from these measurements using the average pressure at tower base as a reference. D. E. Wolfe et al., 2013, (Summary of meteorological conditions during the 2011 Nitrogen, Aerosol Composition and Halogens on a Tall Tower (NACHTT) Experiment, submitted to *Journal of Geophysical Research*, 2013) provide a more detailed description of the meteorological measurements. The sum of these instruments and associated support equipment and consumables (e.g., compressed gases, liquid nitrogen) was equal to the maximum payload and space capacity of the PISA. Air samples were drawn through inlets that extended to a length of approximately 18" (45 cm) mounted on the outside corners (i.e., away from the tower) of the PISA. Instrument exhausts were routed through a 10 m exhaust hose that extended below one corner of the PISA during vertical profiling, and that was attached to a longer exhaust hose and blower during fixed height sampling at ground level.

[23] In addition to the PISA-based instruments, vertical profiles of speciated VOCs were sampled with canisters filled manually at fixed heights accessed from the personnel elevator interior to the tower. A portable sampling manifold was used to fill canisters to ~30 psig using a single head metal bellows pump two to three times per day at heights of 50, 100, 150, 200, and 250 m on the tower throughout the campaign. Additionally, whole air samples were collected hourly from a height of 22 m on the tower from 18 February to 13 March 2011. A total of 90 VOCs were measured from the canister samples, which included C_2–C_{10} nonmethane hydrocarbons, C_1–C_2 halocarbons, C_1–C_5 alkyl nitrates, oxygenated volatile organic compounds, and reduced sulfur gases. Over the course of the campaign, 168 profile samples and 550 hourly samples were collected. Further details regarding the sample collection and laboratory analysis are described in R. F. Swarthout et al., 2013, (Volatile organic compound distributions during the NACHTT campaign at the Boulder Atmospheric Observatory: Influence of urban and natural gas *Journal of Geophysical*

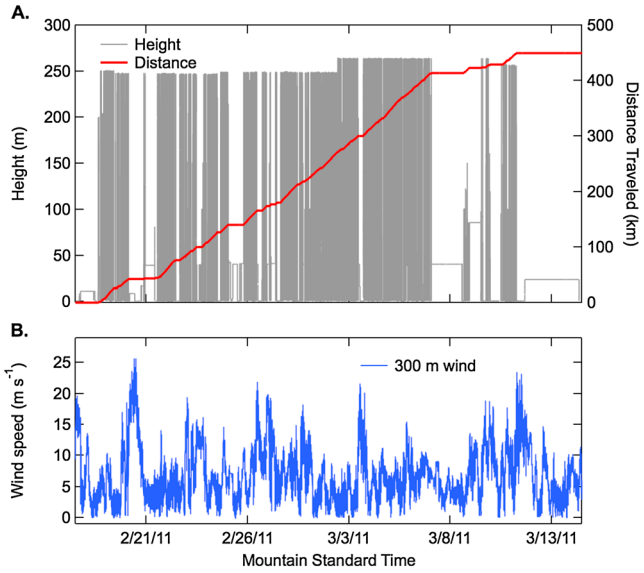

Figure 2. (a) Time series showing carriage height above ground level (left axis) and cumulative distance traveled (right axis). There were a total of 1928 individual profiles, spanning a total distance of ~450 km, over the course of the campaign. (b) Wind speed at 300 m. Vertical profiling was not conducted for winds greater than 12 m s^{-1}.

Research, 2013) and Y. Zhou et al. (Short-lived halocarbons at Boulder Atmospheric Observatory during NACHTT 2011, submitted to *Journal of Geophysical Research*, 2013).

[24] Although PISA was capable of vertical profiling or fixed-height measurements at arbitrary levels, the primary measurement strategy was continuous vertical profiling when possible. Breaks from vertical profiling occurred either for instrument maintenance or for inclement weather conditions. The carriage was not operated during conditions with winds in excess of 12 m s^{-1}. It also could not be operated during conditions when ice formed on the tower surfaces due to loss of contact between the electric bus bars on the tower and the drive motor on the carriage.

[25] Figure 2 depicts the time series of carriage height above ground level. Dense gray lines in the figure indicate periods of continuous vertical profiling, which was relatively consistent during the first two weeks of the campaign. During some periods of higher winds aloft but lower surface winds, vertical profiling was only conducted to 100 m. Profiling was suspended for instrument maintenance for a 1–2 h period each day. The timing of these breaks shifted during each week of the campaign to ensure that the gaps in vertically resolved measurements did not occur at the same time of day for the entire campaign.

3.2. Fixed-Height Measurements of Soluble Trace Gases and Aerosols

[26] Soluble trace gases and ionic and elemental constituents of aerosols were sampled through inlets deployed on a fixed platform at 22 m above ground level (Table 2). Briefly, soluble gases (HCl, HNO_3, HONO, NH_3, HCOOH, and CH_3COOH) were sampled over 2 h intervals by drawing unmodified air at 1.2 m^3 min^{-1} from the level of the platform through a passivated plenum to the base of the tower where the air stream was subsampled at 16 L min^{-1} through a size-fractionating inlet and particle filter followed by tandem mist chambers containing deionized water [*Keene et al.*, 2009; *Russell et al.*, 2003; A. H Young et al., Phase partitioning of soluble trace gases with size-resolved aerosols in near-surface continental air over northern Colorado, USA during winter, submitted to *Journal of Geophysical Research*, 2013]. Exposed mist solutions were analyzed on site by high-performance ion chromatography (IC) usually within an hour after recovery. The ionic composition of size-segregated aerosol (eight fractions with geometric mean diameters ranging from 28 to 0.18 μm) and bulk aerosol was characterized in parallel over daytime (sunrise to sunset) and nighttime (sunset to sunrise) intervals. Ambient air was drawn through a custom designed and fabricated Liu-Pui type inlet and nozzle assembly, and aerosols were size segregated downstream with a MSP Corp. model 130 hi-flow (100 L min^{-1}) cascade impactor configured with polycarbonate substrates and a quartz-fiber backup filter (Young et al., submitted manuscript, 2013). Bulk aerosol was sampled at an average flow rate of 1.3 m^3 min^{-1} on upward facing 20.3 × 25.4 cm Whatman 41 cellulose filters protected by a Lucite "hat" [*Keene et al.*, 2009; *Prospero et al.*, 1989; Young et al., submitted manuscript, 2013]. Following exposure, impaction substrates, backup filters, and bulk filters were stored frozen and subsequently analyzed for 13 ionic constituents via IC at UVA. Subsections of the bulk filters were shipped frozen to UNH for analysis of elemental constituents as summarized below. Bulk aerosol was also sampled over nominal 3 h intervals at an average flow rate of 72 L min^{-1} with downward facing 47 mm filterpack assemblies configured with Whatman 41 cellulose filters [*Lawler et al.*, 2009]. Following exposure, the bulk filters were stored frozen, processed at UNH, and subsequently analyzed for seven elements by neutron activation (NAA) at the Rhode Island Nuclear Science Center (this issue). All pumps were deployed in a vented enclosure at the base of the tower.

3.3. Near-Surface Measurements

[27] A separate set of instruments, housed in trailers located immediately south of the main tower, provided near-surface measurements of VOCs, ozone, hydroxyl radicals (OH), hydrochloric acid (HCl), and actinic flux (Table 3). Inlets for the VOC measurements were mounted on the scaffolding tower at 9 m above ground level. A suite of 43 speciated VOCs including primary emissions (alkanes, alkenes, aromatics) and oxygenated species was measured with an in situ GC-MS instrument [*Gilman et al.*, 2009] deployed at the base of the tower. This instrument analyzed one sample every 30 min with a 5 min integration time per sample. A set of 14 VOCs, principally aromatics and oxygenates, was measured in parallel with a time-of-flight proton transfer reaction mass spectrometer and reported at 1 min time resolution. A commercial UV ozone monitor recorded mixing ratios of ozone at 1 min time resolution from the same inlet. Concentrations of hydroxyl radical, OH, were measured by CIMS via conversion of OH to isotopically labeled sulfuric acid [*Tanner et al.*, 1997]. This instrument sampled directly through the trailer wall at a height of 2 m above ground level. It was operational for approximately the first two weeks of the three-week campaign. A near-infrared CRDS measured ambient mixing ratios of hydrochloric acid, HCl, again from an inlet that extended directly through the trailer wall at a height of 2 m. Last, filter radiometers mounted on top of the 9 m scaffolding tower recorded photolysis frequencies for O_3 (to produce $O(^1D)$), NO_2 and NO_3 with 1 min time resolution

Table 2. Soluble Trace Gas and Aerosol Components at 22 m Height

Species/Parameter	Reference	Method	Sample Time	Detection Limit (DL)	Uncertainty
Soluble trace gases	*Keene et al*., [2009]	MC/IC[a]	2 h	HCl: 23 pptv HNO_3: 45 pptv HONO: 32 pptv NH_3: 1.43 ppbv HCOOH: 455 pptv CH_3COOH: 575 pptv	±5% to ±15% or ±0.5*DL whichever is the greater absolute value
Ionic composition of size-resolved aerosols (eight size fractions; GMD[b] 28 to 0.18 μm)	Young et al. (submitted manuscript, 2013)	Cascade Impactor/IC[c]	~12 h	***Seven larger fractions*** CH_3COO^-: 0.097 nmol m^{-3} $HCOO^-$: 0.133 nmol m^{-3} $(COO)_2^{2-}$: 0.014 nmol m^{-3} $CH_3SO_3^-$: 0.028 nmol m^{-3} SO_4^{2-}: 0.015 nmol m^{-3} Cl^-: 0.015 nmol m^{-3} Br^-: 0.001 nmol m^{-3} NO_3^-: 0.005 nmol m^{-3} NH_4^+: 0.168 nmol m^{-3} Na^+: 0.071 nmol m^{-3} K^+: 0.015 nmol m^{-3} Mg^{2+}: 0.001 nmol m^{-3} Ca^{2+}: 0.003 nmol m^{-3} ***Smallest fraction*** CH_3COO^-: 0.268 nmol m^{-3} $HCOO^-$: 0.337 nmol m^{-3} $(COO)_2^{2-}$: 0.005 nmol m^{-3} $CH_3SO_3^-$: 0.324 nmol m^{-3} SO_4^{2-}: 0.044 nmol m^- Cl^-: 0.119 nmol m^{-3} Br^-: 0.011 nmol m^{-3} NO_3^-: 0.021 nmol m^{-3} NH_4^+: 0.483 nmol m^{-3} Na^+: 0.158 nmol m^{-3} K^+: 0.046 nmol m^{-3} Mg^{2+}: 0.020 nmol m^{-3} Ca^{2+}: 0.133 nmol m^{-3}	
Ionic composition of bulk aerosol	*Keene et al*., [2009]	Hi vol/IC[d]	~12 h	CH_3COO^-: 2.05 nmol m^{-3} $HCOO^-$: 2.69 nmol m^{-3} $(COO)_2^{2-}$: 0.029 nmol m^{-3} $CH_3SO_3^-$: 0.004 nmol m^{-3} SO_4^{2-}: 0.048 nmol m^{-3} Cl^-: 0.389 nmol m^{-3} Br^-: 0.029 nmol m^{-3} NO_3^-: 0.183 nmol m^{-3} NH_4^+: 9.40 nmol m^{-3} Na^+: 0.305 nmol m^{-3} K^+: 0.396 nmol m^{-3} Mg^{2+}: 0.035 nmol m^{-3} Ca^{2+}: 0.133 nmol m^{-3}	<±5% or 0.5*DL whichever is the greater absolute value
Elemental composition of bulk aerosol	*Lawler et al*., [2009]	Hi vol/NAA[e]	~12 h	Na: 0.33 nmol m^{-3} Mg: 0.08 nmol m^{-3} Al: 0.04 nmol m^{-3} Cl: 0.7 nmol m^{-3} Mn: 0.002 nmol m^{-3} V: 0.002 nmol m^{-3} Br: 0.019 nmol m^{-3}	7–11 %
Elemental composition of bulk aerosol	*Lawler et al*., [2009]	FP/NAA[f]	~3 h	Na: 2.9 nmol m^{-3} Mg: 0.74 nmol m^{-3} Al: 1.0 nmol m^{-3} Cl: 2.8 nmol m^{-3} Mn: 0.001 nmol m^{-3} V: 0.002 nmol m^{-3} Br: 0.015 nmol m^{-3}	5–9 %
Speciated VOCs	*Russo et al*., [2010]; *Sive et al*., [2005]; *Zhou et al*., [2008]	Canister samples, GC-MS analysis	two to three times/day	<10 pptv	NMHC 1–8% Alkyl nitrates 3–8% Halocarbons 4–15%

[a]Sampled with tandem Mist Chambers and analyzed by IC.
[b]Ambient Geometric Mean Diameter.
[c]Sampled with custom MSP corp. model 130 high flow Cascade Impactor and analyzed by IC.
[d]Collected with high-volume bulk sampler and analyzed by IC.
[e]Collected with high-volume sampler and analyzed by NAA.
[f]Sampled with Filter Packs and analyzed by NAA.

Table 3. Near-Surface Instruments

Species/Parameter	Reference	Method	Sample Frequency	Detection Limit	Uncertainty
Speciated VOC	*Gilman et al.*, [2009]	GC-MS	5 min sample every 30 min	0.5 – 10 pptv	15%
O_3	*Williams et al.*, [2006]	UV absorption	1 min	1 ppbv	3%
OH	*Tanner et al.*, [1997]	CIMS	10 min	10^5 molecules cm^{-3}	35%
HCl	C. L. Hagen et al. 2013, (Cavity ring-down spectroscopy sensor for detection of hydrogen chlorids, submitted to *Atmospheric Measurement Techniques*, 2013)	CRDS	1 min	20 pptv	10%
Photolysis frequencies	*Stark et al.*, [2007]	Filter radiometers	1 min		14%

[*Stark et al.*, 2007]. Photolysis rates for other gases, such as HONO and $ClNO_2$, were calculated based on the measured photolysis rates from previously published comparisons between filter radiometer and wavelength resolved spectroradiometer measurements [*Young et al.*, 2012].

4. Data Overview: Ozone, Nitrogen Oxides, and Radical Reservoirs

[28] The NACHTT data set is complex because it includes chemical composition of gas and aerosol species as a function of both time and height above ground level. In addition, meteorological conditions during the campaign were highly variable, with relatively stagnant, polluted periods interspersed with cleaner periods associated with strong westerly downslope flow along the Rocky Mountain foothills to the west of the site. Wolfe et al. (submitted manuscript, 2013) review the meteorological observations during NACHTT.

[29] Figure 3 shows O_3, NO_2, and NO for the entire three-week campaign at 1 s time resolution. The highest ozone was 50–55 ppbv, observed during cleaner periods associated with strong westerly flow. Ozone was generally higher at the top of the tower, especially at night. Lower ozone values were observed during polluted, higher NO_x conditions, consistent with titration of ozone by local NO_x emissions. The variability in ozone apparent in the figure is largely due to vertical profiling, as indicated by the carriage height time series at the bottom of the figure. Variability with height was most pronounced during nighttime (see below). Average ozone for the entire campaign was 37 ± 13 ppbv. Elevated levels of NO_x pollution were most commonly observed near the surface, but were also occasionally present in lofted plumes at night. Nitrogen dioxide (NO_2) varied from 50 pptv to 50 ppbv, the limit associated with full titration of the background ozone levels. There were occasional, intense, transient nitric oxide plumes of several tens of parts per billion, with a maximum value of 105 ppbv. These intense plumes were sometimes observed at surface level, and sometimes in layers aloft at night. Minimum NO_x during periods of strong westerly winds was 50 – 70 pptv. Average NO_x for the entire data set was 6.9 ± 9.1 ppbv (relative standard deviation of 130%). Median NO_x was 3.7 ppbv, with 25th and 75th percentiles of 1.5 and 8.1 ppbv, respectively, and 10th and 90th percentiles of 0.6 and 16.7 ppbv, respectively.

[30] The vertical variation of trace gases with time of day is more readily apparent from an expanded view of a single day's data. Figure 4 shows O_3 and NO_x for one diurnal cycle (1–2 March), during which vertical profiling was nearly continuous. Winds on 1 March were from the east or southeast and relatively strong ($4\,m\,s^{-1}$ at 10 m, $8\,m\,s^{-1}$ aloft), but shifted to northerly near 8 PM on 1 March, varying between 1 and $6\,m\,s^{-1}$ for the remainder of the time series. Ozone decreased at all altitudes after the wind shift, and NO_x became more concentrated, most likely due to a reduction in wind speed. The top panel shows the data as time series, including tower carriage height and solar elevation angle, to indicate the frequency of profiling and the time of day. The bottom two panels show the same data plotted as height versus time, color coded by O_3 and NO_x, respectively. These panels give a detailed view of the variation in these species with height and time of day, and show the clear anticorrelation between NO_x and O_3 for this winter, urban-influenced air. During daylight hours on 1 March, all species were well mixed and invariant with tower carriage height. Shortly after sunset, however, the variations in NO_x and O_3 with height become apparent, with ± 30 ppbv variations in O_3 and ± 20 ppbv

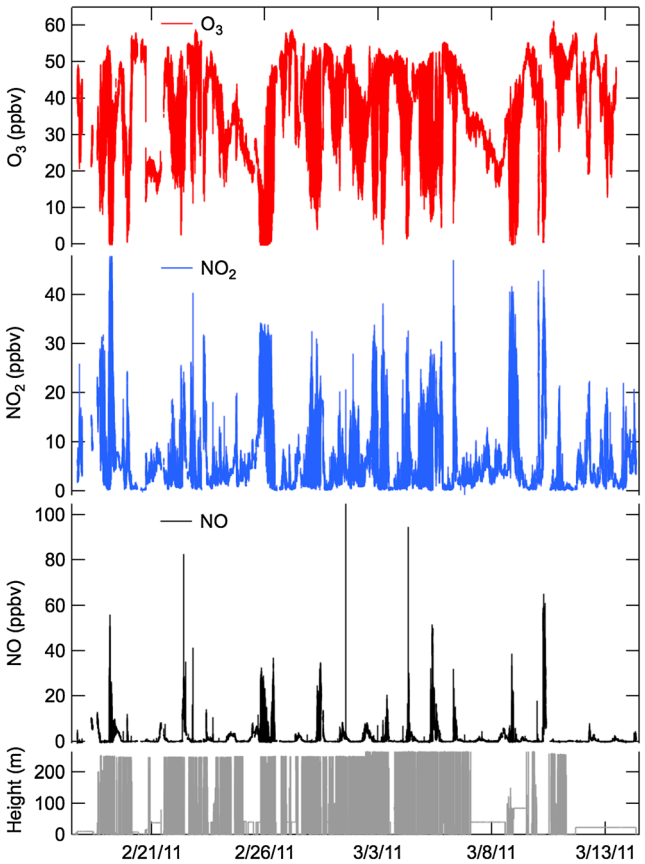

Figure 3. Time series of ozone, NO_2, and NO at 1 s time resolution from the tower carriage for the NACHTT campaign. The bottom panel shows the time series of height to indicate periods when the carriage was profiling.

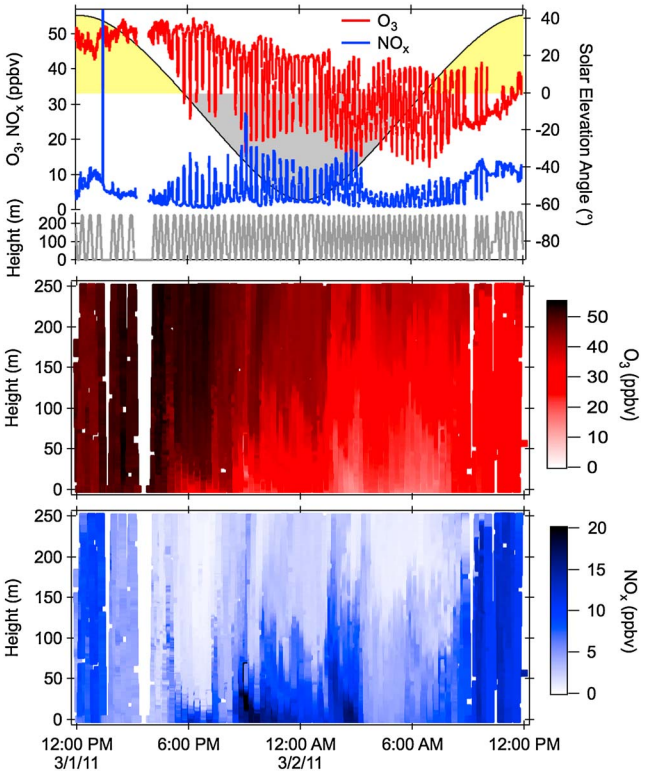

Figure 4. Expanded view of a single day of measurement on which vertical profiling was almost continuous (data gap in late afternoon of 1 March for instrument maintenance). (top) The time series of O_3 and NO_x, plotted together on the same axis (left), solar elevation angle (right axis), and tower carriage height (lower left axis). (middle and bottom) Height versus time, color coded by O_3 and NO_x, respectively (see color scales at right). The color plots show the variation and anticorrelation of these species with height and time.

variations in NO_x. Vertical variations persisted for approximately 3.5 h after sunrise (6:40 AM) on 2 March. Mixing took place from bottom to top, with growth in a mixed layer of NO_x and O_3 beginning at low altitude near 8 AM and continuing through 10:15 AM, when the entire 250 m column was mixed. Thus, at this time of year (late winter) at this location, the lower atmosphere was mixed from approximately 3 h after sunrise until approximately sunset, or approximately 7.5 h of the 11 h of daylight. Other days exhibited similar timing in the duration of mixing.

[31] Odd oxygen ($O_x = O_3 + NO_2$) was not conserved on these vertical profiles and was lower at the bottom of profiles than at the top during nighttime hours. Figure 5 shows the extent of the vertical variability in O_x for the 1–2 March diurnal cycle. Vertical gradients in O_x were as large as 25 ppbv at times. Inclusion of the odd oxygen reservoir in N_2O_5 (i.e., nocturnal odd oxygen $= O_3 + NO_2 + 3N_2O_5$ [*Brown et al.*, 2006a]) did not reduce the magnitude of the gradients; indeed, since N_2O_5 was tended to be small at the bottom of the profiles, but larger at the top, gradients in nocturnal odd oxygen ($O_3 + NO_2 + 3N_2O_5$) were in general modestly larger than those of conventional O_x ($O_3 + NO_2$). Ammonium nitrate aerosol, the major end product from the heterogeneous hydrolysis of N_2O_5 in this environment, was enhanced at the bottom of the profile. Gas-phase nitric acid was small in comparison and did not have gradients that were nearly as distinct. Inclusion of the odd oxygen contained in ammonium nitrate (i.e., $O_3 + 2NO_2 + 3N_2O_5 + 1.5NO_3^-$, not shown) reduced the O_x gradients by 5–15%. These observations are consistent with some loss of odd oxygen to ammonium nitrate aerosol production and some to dry deposition of ozone at the ground surface. However, without a measurement of total reactive nitrogen or an estimate of dry deposition rates for ozone, ammonium nitrate, and gas-phase nitric acid, the relative contributions to odd oxygen loss in the boundary layer are difficult to determine quantitatively. Gradients in odd oxygen of similar magnitude to those from 1–2 March were apparent on many nights with continuous vertical profiling and low surface wind speeds.

[32] Variations of NO_x and O_3 with height, wind direction, and time of day further illustrate the mix of background air and pollutants that influence the Front Range. Figures 6 and 7 show the median, and 10th, 25th, 75th, and 90th percentile mixing ratios of NO_x and O_3 in different height intervals for day and night. Nighttime is defined as sunset to 2.5 h after sunrise, the average time of day at which the 10 m and 100 m temperatures became equal. This definition divides well mixed versus stratified air masses rather than sunlit and dark. Data are also filtered for wind speeds less than 7.7 m s^{-1}. This wind speed is the 2σ value of a Gaussian fit to a histogram of wind speeds and is intended to exclude the influence of very high wind events associated with downslope flow along the Rocky Mountain foothills. The filter excludes 6.5% of the data. Nighttime O_3 variability is largest in the lowest height interval and decreases steadily with height, with percentiles, and the median for 100–270 m encompassing a tight range. The major exception is south-southwest flow in the 100–270 m interval, where the influence of O_3 titration due to large plumes of NO_x from the urban area is apparent (also see Figure 7). Smaller O_3 titrations are evident in other

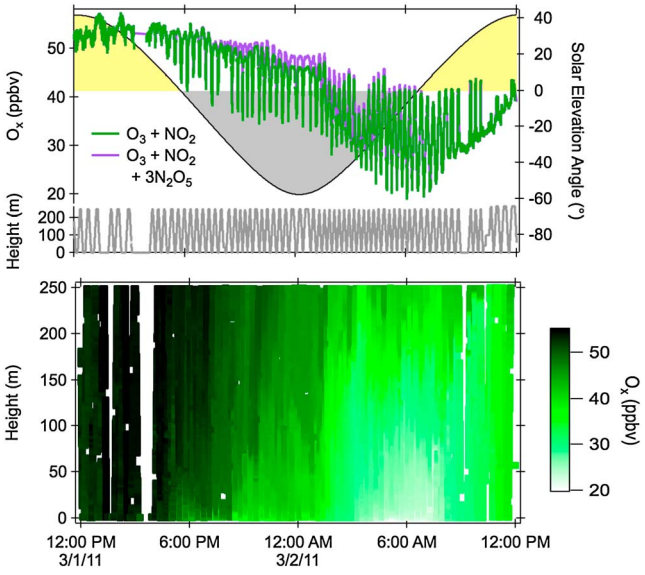

Figure 5. Expanded view of odd oxygen for 1–2 March. (top) The time series of O_x, calculated both as $O_3 + NO_2$ (green) and as $O_3 + NO_2 + 3N_2O_5$ (violet). (bottom) A color plot of O_x ($O_3 + NO_2$) as a function of height above ground level.

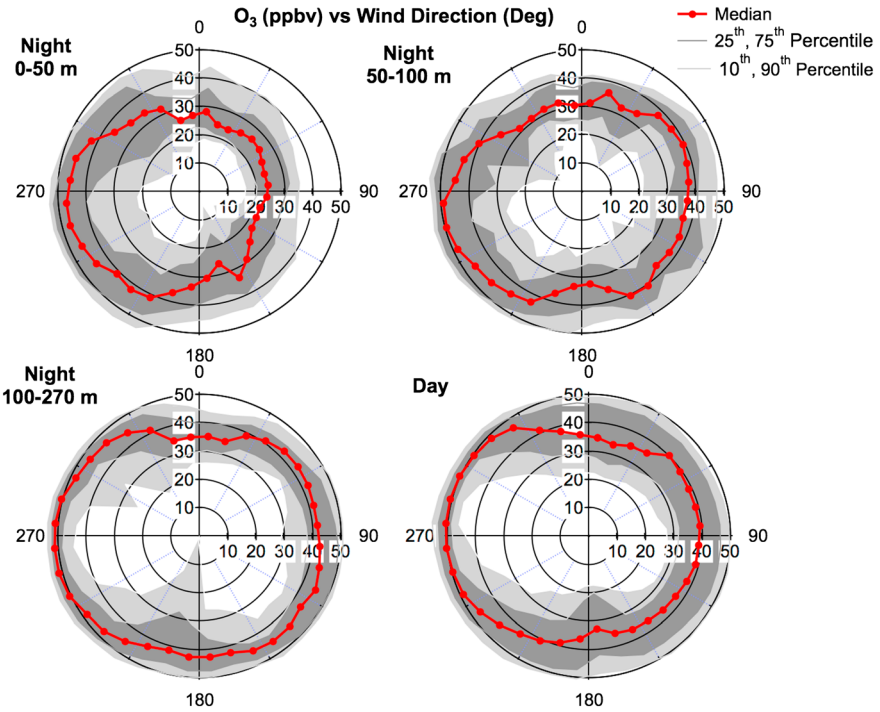

Figure 6. Wind rose plot of O_3 statistics in different height intervals and times of day. Largest variations occurred at night and below 100 m. The top two plots show nighttime data for 0–50 and 50–100 m. The bottom two plots show nighttime data for 100–270 m and all daytime data, irrespective of height. Nighttime is defined as sunset to 2.5 h after sunrise, the period when the boundary layer was not well mixed (see text). Red points and lines in all plots are median values, dark shading is 25th and 75th percentiles, and light shading is 10th and 90th percentiles. Data are filtered to exclude wind speeds greater than 7.7 m s^{-1}, which are high-wind, downslope events.

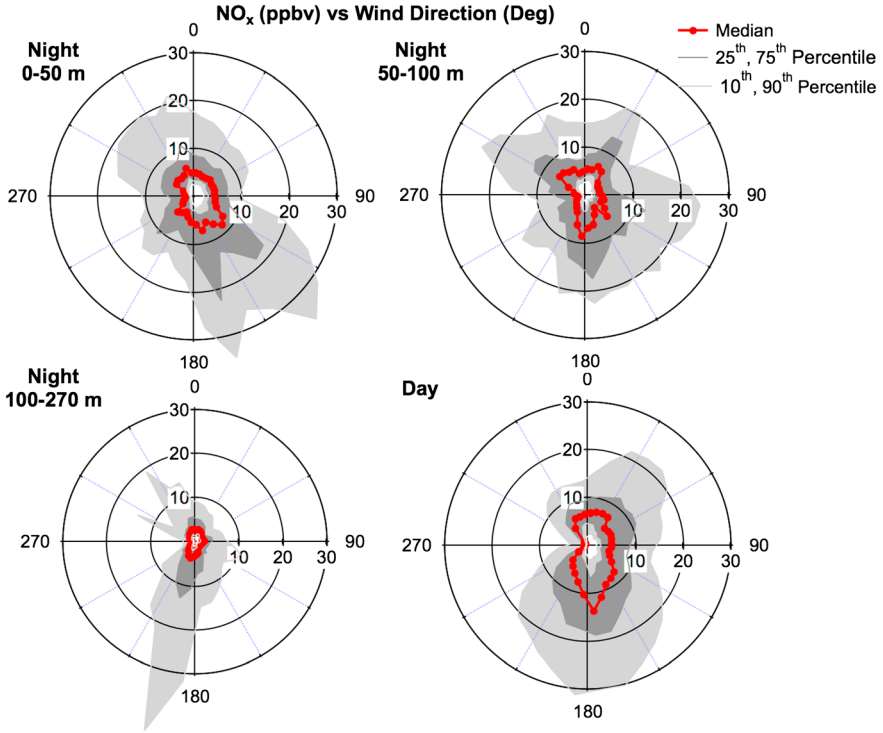

Figure 7. Same as Figure 5, except showing statistics for NO_x rather than O_3.

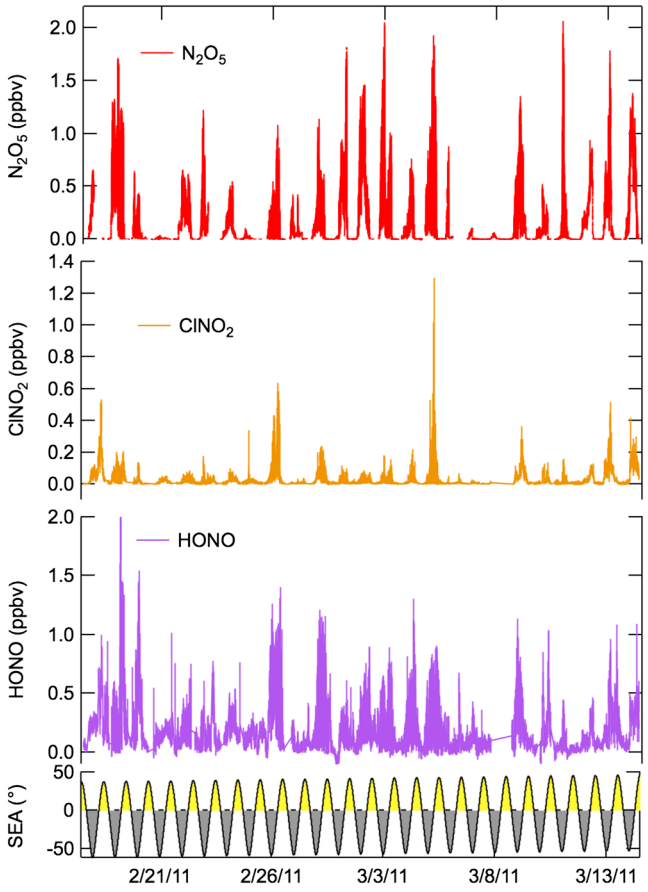

Figure 8. Time series of N_2O_5, $ClNO_2$, and HONO for the NACHTT campaign. All data are at their native time resolution (1 s for N_2O_5, 10 s for $ClNO_2$ and HONO). The lower panel shows solar elevation angle to distinguish day from night and to illustrate the day/night variation over the course of the campaign.

wind sectors as well. Similarly, O_3 levels are highest and variability smallest for westerly or west southwesterly flow at all elevations and times of day. These observations are consistent with the influence of higher background O_3 transported into the region from the west, and O_3 titration or destruction due to the input of pollution from the urban area at low altitude at night, or from wind directions other than west. Particularly during daytime, the larger median O_3 value and smaller range of variability is apparent in westerly relative to easterly flow. Statistics for NO_x in Figure 7 show related trends. Variability is largest at low altitude during nighttime, but mixing ratios and variability are a much stronger function of wind direction for NO_x than for O_3. All wind roses show a maximum for southerly flow from the Denver urban area, although the exact direction of the maximum and its magnitude and variability are different for each rose. For example, low altitude nighttime data show a strong maximum and large variability for southwesterly flow, from the direction of both the Denver urban area and the industrial areas on the west side of Denver. Nighttime NO_x at high altitude has an extremely pronounced maximum, likely from buoyant plumes of either urban or industrial origin, although the direction is slightly east of south, not directly towards major NO_x point sources (e.g., see large power plant location in Figure 1). Titration of O_3 due to these plumes is also apparent in the nighttime 100 to 270 m wind rose in Figure 6. The NO_x wind roses indicate that Denver is the largest NO_x source in the area, but not the only one. Secondary maxima are apparent during northeasterly flow at night in the 50 to 100 m range and during daytime.

[33] Finally, Figure 8 shows the time series and comparison of the two major nighttime radical reservoir species, $ClNO_2$ and HONO, along with the $ClNO_2$ precursor, N_2O_5. Papers by N. L. Wagner et al. (N_2O_5 uptake coefficients and nocturnal NO_2 removal rates determined from ambient wintertime measurements, submitted to *Journal of Geophysical Research*, 2013), T. P. Riedel et al. (Chloride plumes and point sources in the Denver urban area in wintertime: Vertically resolved ClNO2 measurements, submitted to *Journal of Geophysical Research,* 2013) and T. C. VandenBoer et al. (Understanding the role of the ground surface in HONO vertical structure: High resolution vertical profiles during NACHTT-11, submitted to *Journal of Geophysical Research*, 2013) examine the detailed characteristics of N_2O_5, $ClNO_2$, and HONO, respectively. All three species varied on similar mixing ratio scales, between approximately 0 and 2 ppbv over the duration of NACHTT. The diurnal variation in N_2O_5 and $ClNO_2$ is readily apparent. As in the previous work on N_2O_5 and $ClNO_2$ from the Kohler mesa site west of BAO [*Thornton et al*., 2010], $ClNO_2$ was observed in nearly every nighttime urban plume in which N_2O_5 was also present, but the relative amounts of N_2O_5 and $ClNO_2$ varied greatly. The large variability within any given night for either of these species resulted largely from the dependence on height during vertical profiling of the tower carriage (see above). Nitrous acid, HONO, also shows large diurnal variation and variability within any given night. Its levels are more persistent than those of $ClNO_2$, indicating that its photolysis was a larger source of radicals. The above referenced papers and the discussion below examine these issues in more detail.

5. Overview of Results

[34] This section presents an overview of the some of the important results of the NACHTT field study, including those published in this special journal section, published elsewhere, and emerging in manuscripts that are still in preparation.

5.1. Meteorology

[35] Meteorology along the Front Range urban corridor and the eastern plains of Colorado plays a key role in air pollution events that trap emission from various sources within the air shed adjacent to the Rocky Mountains. The analysis of Wolfe et al. (submitted manuscript, 2013) identifies four major weather patterns that impact winter Front Range air quality generally and the NACHTT campaign specifically. The first was nocturnal drainage flow, generally from southwest to northeast along the South Platte River valley, which transports urban emissions from Denver to the BAO site and locations to the north and east. The second was upslope winds, generally from the northeast, towards the Rocky Mountain foothills. This flow is often thermally driven (i.e., daytime), but can also occur under dynamical influence at any time of day, and leads to a concentration of pollutant emissions within the urban area. The third pattern was moist, cool upslope winds associated with storm systems to the

southeast of the site or to high pressure on the plains to the northeast. This pattern often leads to precipitation, but during NACHTT resulted mainly in fogs and low clouds. It was responsible for the rime ice event that suspended vertical profiling at the tower during 7–9 March (see Figure 2). Finally, the region is also subject to strong downslope westerly winds events near the Rocky Mountain foothills. These events occurred periodically during NACHTT and served to significantly reduce the measured levels of urban and other pollutants.

[36] In general, meteorology during NACHTT was drier than normal, with no precipitation events during the study. There were also no major cold weather events, as the storm track during the period was generally to the north of the study area, such that most cold fronts only clipped the study area.

5.2. Soluble Trace Gases and Aerosols

[37] A key motivation for NACHTT was to understand the cycling and partitioning of chlorine and chloride species. Previous field measurements of halogen activation processes through $ClNO_2$ have invoked a chloride reservoir in the form of HCl in order to justify the observed balance between $ClNO_2$ and particulate chloride, since measured $ClNO_2$ has been reported in large excess over submicron chloride [*Osthoff et al*., 2008; *Thornton et al*., 2010]. Key issues identified in the understanding of chloride partitioning between the gas and aerosol phases included measurements of size-resolved composition, the aerosol hydration state, and aerosol pH. Young et al. (submitted manuscript, 2013) report measurements from a fixed height at 22 m of soluble trace gases (HCl, HNO_3, and NH_3) and aerosol composition (NO_3^-, SO_4^{-2}, NH_4^+, Na^+, Cl^-) for eight discrete size bins between 0.18 and 28 μm ambient geometric mean diameter. Aerosol liquid water content was calculated using a thermodynamic model, and aerosol solution pH was inferred from the observed partitioning of different gas and aerosol phase pairs (e.g., NO_3^- and HNO_3, Cl^- and HCl). Principal conclusions of this analysis were as follows. First, the sum of gas-phase HCl and particulate chloride was always in excess of measured $ClNO_2$ in near-surface air. Condensation of HCl prevented depletion of particulate chloride via $ClNO_2$ production at night. These results demonstrate for the first time a chloride balance sufficient to explain the degree of observed halogen activation through $ClNO_2$. Interestingly, however, the majority of the chloride mass was present in the supermicron size range, and was almost entirely associated with sodium. Smaller but persistent gas-phase HCl (median 72 pptv) and submicron chloride were also observed. Second, the diurnal variation of both gas-phase HCl and HNO_3 showed a maximum during daytime, with the daytime HCl maximum more pronounced than that of HNO_3. This result is consistent with photochemical generation of stronger acids (presumably sulfuric) that displaced HCl and HNO_3 from the particulate phase and with the diurnal temperature variation. RHs and associated aerosol water contents were also significantly lower during daytime relative to night and the corresponding variability in phase partition contributed to the observed diel variability in HCl and HNO_3. Finally, development of the nocturnal inversion contributed to depletion of HCl and HNO_3 in near-surface air via deposition to the surface at night. Subsequent ventilation following sunrise and associated mixing with undepleted air from aloft would have also contributed to diel variability. Third, aerosol pH calculated from partitioning of gas and aerosol species was in the range <1 to 4, and had a smaller increase in pH with particle size than marine influenced regions. Interestingly, pHs inferred from HNO_3/NO_3^- and NH_3/NH_4^+ were similar whereas those inferred from HCl/Cl^- were typically higher by 1 to 2 pH units. These differences probably reflect bias in the Henry's law constant for HCl used in the calculations but fall within the uncertainty bounds corresponding to the wide range of Henry's Law constants for HCl reported in the literature. Fourth, detectable levels of aerosol bromide were typically observed. Despite the relatively low concentrations, bromine chemistry may still be important to halogen activation and radical recycling, and should be considered in models, even in continental regions. Finally, the sources of the observed chloride were not clear, but the association with sodium suggested either long-range transport of marine air (1 to 2 days from the U.S. West Coast), aerosol generation over playas or other mineral sources in areas in the U.S. intermountain west, or a local source from road salting. The latter source was uncertain since there were no snowfall events, and thus no road salting activity, during the campaign. Young et al. (submitted manuscript, 2013) do not explicitly consider chloride from combustion sources, such as coal [*McCulloch et al*., 1999], though T. P. Riedel et al. (Chloride plumes and point sources in the Denver urban area in wintertime: Vertically resolved ClNO2 measurements, submitted to *Journal of Geophysical Research,* 2013) do consider this source in a separate paper prepared for this issue (see below).

[38] One of the key questions raised by the presence of halide salts and gas-phase, photolabile halogen species is the degree of marine influence on the sampled air masses. Halocarbon compounds are often used as tracers for marine air. Zhou et al. (submitted manuscript, 2013) analyzed measurements of seven different compounds (CH_2Cl_2, $CHCl_3$, C_2HCl_3, C_2Cl_4, $CHBr_3$, CH_2Br_2, CH_3I) to ascertain their local versus long-range contributions during NACHTT. All of these compounds are considered short lived since their atmospheric lifetimes are on the order of six months or less. All of the chlorinated compounds are solvents used for industrial purposes and exhibited relatively large mixing ratios and variability during NACHTT. Chloroform, $CHCl_3$, is also associated with emissions from water treatment and was at times not well correlated with the other chlorine compounds, but was well correlated with $CHBr_3$. The brominated species and methyl iodide all exhibited much lower concentrations, on the low end of previously reported mixing ratios from tropospheric measurements. All compounds were more enhanced at night and during southerly wind flow, indicating a local, rather than a marine source. Vertical distributions corroborated this finding. On this basis, the authors infer very little marine influence to the sampled air, indicating that the chloride source in other measurements may not be due to long-range transport from marine areas. The analysis also included flux estimates for chlorinated and brominated compounds that were similar to, but slightly lower than, per capita inventories for halocarbon emissions in the U.S.

[39] Deployment of an AMS on the tower carriage during NACHTT provided vertically resolved measurements of submicron aerosol composition. Although there is now a large body of literature from AMS measurements in various locations, the majority of these data is from warm (summertime) conditions and does not include vertically resolved measurements. The analysis of F. Özturk et al. (Vertically resolved

chemical characteristics and sources of sub-micron aerosols in a suburban area near Denver, Colorado in winter, submitted to *Journal of Geophysical Research,* 2013) (this issue) showed that aerosol mass loadings were generally largest below 120 m height, where the Denver urban plume was concentrated. Average mass loadings during NACHTT were 4.6 μg m^{-3}, although peak loadings during stagnation events were in the range 20 to 30 μg m^{-3}. Consistent with some of the more recent winter measurements in the Denver air shed, the AMS measurements showed nitrate to be the dominant component of aerosol mass loading (35%), but that contributions from organic (26%), sulfate (20%), and ammonium (17%) were appreciable. Nonrefractory chloride was a minor but consistent component of submicron aerosol, with an average contribution of 1%. The OA component was further subdivided using positive matrix factorization analysis into two oxidized OA (OOA) components (OOA I, aged and more oxidized; OOA II, less aged and less oxidized) and a hydrocarbon-like OA (HOA, much less oxidized, primary emission). The OOA I component was found to correlate well with sulfate and nitrate, while OOA II was correlated with nitrate and HOA was well correlated with gas-phase nitrogen oxides (NO_x). Wind rose analysis of the near-surface data (below 40 m) showed an association between high daytime aerosol mass loadings and low wind speeds (stagnant conditions). At night, high aerosol mass loading was associated with transport from urban Denver to the southeast and to a lesser extent with transport from ammonia rich regions to the northeast (see Figure 1). Data between 40 and 120 m elevation at higher wind speeds (greater than 4 m s^{-1}) was filtered using a back trajectory cluster analysis to determine the contribution from longer-range transport into the study area. During daytime, sulfate was a dominant aerosol component for air masses associated with the longest distance back trajectories, indicating it was most influenced by long-range transport, while sulfate, nitrate and organic contributed more equally in air masses associated with the shorter-range trajectories. The results were consistent with the correlation between sulfate and OOA I, which is the aged and oxidized component of OA.

5.3. Heterogeneous Nitrogen Oxide Processes and OH

[40] A key goal of NACHTT was to understand the role of heterogeneous nitrogen oxide reactions in both the removal of NO_x from the atmosphere and in the activation of oxidants such as Cl and OH. Toward that end, four separate analyses from NACHTT examined (1) the efficiency of heterogeneous nitrogen oxide uptake, its dependence on aerosol composition and its role in NO_x loss; (2) ambient levels of $ClNO_2$ arising from N_2O_5 uptake to chloride-containing aerosol, the distribution of $ClNO_2$ with height above ground and the efficiency of $ClNO_2$ production from different source sectors; (3) the vertical distributions and diurnal behavior of HONO, the implications for process level chemistry behind its production, and the influence of HONO on radical production; and (4) the ambient levels of OH at surface level and the comparison to predictions from a model, including the influence of HONO and photo-labile chlorine.

[41] Heterogeneous uptake of N_2O_5 is the primary mechanism for nitrogen oxide loss in winter [*Dentener and Crutzen*, 1993]. A key parameter required by atmospheric models to understand this process is the N_2O_5 uptake coefficient, $\gamma(N_2O_5)$, or the probability of reactive uptake per gas-particle collision. Together with the aerosol surface area density (S_A), the uptake coefficient determines the first-order loss rate coefficient for N_2O_5.

$$k(N_2O_5) = \frac{1}{4} c\gamma(N_2O_5) S_A \quad (1)$$

[42] Here c is the mean molecular speed of N_2O_5. There is a growing body of literature determinations of $\gamma(N_2O_5)$ from ambient measurements that have shown wide variability and significant differences from laboratory-based parameterizations [*Bertram et al*., 2009; *Brown et al*., 2006b]. However, nearly all of these determinations have been for summertime and/or warm conditions. Wagner et al. (submitted manuscript, 2013) report determinations of N_2O_5 uptake coefficients, $\gamma(N_2O_5)$, from vertically resolved, wintertime measurements of this compound, nitrogen oxides, ozone, and aerosol size distributions. The approach is an iterative box model to determine $\gamma(N_2O_5)$ at high time resolution (e.g., 1 s, the same as the measurements). Although the box model also has limitations in its validity that limit it to less than 10% of the total nighttime data, the analysis yields approximately 10^5 individual determinations of $\gamma(N_2O_5)$. Key findings from the analysis include the following. First, the determined $\gamma(N_2O_5)$, though spanning a wide distribution, peak in the range 0.01 – 0.02, nearly the range from laboratory determinations for uptake to inorganic substrates [*Chang et al*., 2011]. Although the lower end of the range of determinations extends to values as small as $\gamma(N_2O_5) = 0.002$, a value consistent with previous determinations from summertime, low values are only a small fraction of the data. The determinations show a clear dependence on height that is attributable to the presence of large aerosol nitrate loadings, which are known to suppress $\gamma(N_2O_5)$. However, the suppression is modest, and not sufficient to make heterogeneous N_2O_5 uptake a rate-limiting step in the overall NO_x loss process. Rather, the reaction of NO_2 with O_3 is rate limiting.

$$NO_2 + O_3 \rightarrow NO_3 + O_2 \quad (R3)$$

$$NO_2 + NO_3 \rightleftharpoons N_2O_5 \quad (R4)$$

$$N_2O_5 + \text{aerosol} \rightarrow \text{products}(HNO_3 \text{ or } C1NO_2) \quad (R5)$$

[43] A comparison of integrated nighttime NO_x loss through this reaction scheme to the integrated daytime loss due to reaction of NO_2 with OH (determined from measured OH at surface level, see S. Kim et al. (The primary and recycling sources of OH during the NACHTT-2011 campaign, submitted to Journal of Geophysical Research, 2013) showed both to be strongly dependent on NO_x levels, but that nighttime NO_x loss exceeded the potential range of photochemical loss defined by the OH measurements.

[44] A major motivation for the NACHTT study was the discovery of surprisingly large, midcontinental $ClNO_2$ mixing ratios in winter at a location just west of the BAO tower [*Thornton et al*., 2010]. Although the previous study identified substantial yields (average 17%) and persistence of $ClNO_2$ within the Front Range urban plume, it did not address the question of $ClNO_2$ vertical distributions, which are important at night and during winter. T. P. Riedel et al. (Chloride plumes and point sources in the Denver urban area in wintertime: Vertically resolved ClNO2 measurements, submitted to

Journal of Geophysical Research, 2013) report $ClNO_2$ measurements in plumes from combustion sources observed above surface level during nighttime vertical profiling. There were several instances of intense nighttime nitrogen oxide plumes in the altitude range 50 to 250 m. These plumes were generally associated with either southerly or southwesterly flow at the tower, and may be attributable to urban emission from Denver, or point source emissions from electric power generation or industrial activity in the Denver area. Interestingly, the plumes contained considerable particulate chloride in addition to nitrogen oxides, indicating a common combustion source for both chloride and NO_x. These plumes also had large $ClNO_2$ mixing ratios, ranging from a few hundred parts per trillion to over a part per billion. A box model analysis of the individual plumes suggested N_2O_5 uptake coefficients in the range of 0.008 – 0.015, consistent with the analysis of Wagner et al. (submitted manuscript, 2013), and $ClNO_2$ yields (i.e., $ClNO_2$ produced per N_2O_5 consumed) of approximately 40%. Some plumes also contained Cl_2 at levels of a few tens of pptv. The results suggest that co-emission of NO_x and chloride (likely emitted in the form of HCl) from urban or point source combustion may be an important contributor to halogen activation.

[45] Nitrous acid, HONO, is another nighttime radical reservoir species arising from a heterogeneous process. Nitrous acid is known to have strong vertical gradients during both night and day, and small levels of reported HONO during daytime imply a rapid, photochemical production that may represent a significant OH source (see introduction). Profiles of HONO from the BAO tower provide detailed information with which to assess its vertical distribution and implications for nitrogen oxide and oxidant budgets. VandenBoer et al. (submitted manuscript, 2013) present this analysis for the NACHTT study. Similar to vertically resolved measurements from previous field studies, NACHTT data exhibit strong nighttime vertical gradients in HONO, especially near surface level. Nitrous acid is produced directly from the heterogeneous reaction of NO_2 at surfaces, but its uptake coefficient is much smaller than that for N_2O_5, the precursor to $ClNO_2$. Uptake of NO_2 by the ground surfaces tends to be the dominant pathway for HONO production, whereas uptake of N_2O_5 by aerosols tends to dominate $ClNO_2$ production. Modeling of the NACHTT results also suggests substantial deposition of HONO back to the ground surface, a process that competes with NO_2 uptake to limit the total gas-phase HONO levels. Also similar to previous studies, the NACHTT data show near-surface daytime HONO that is significant enough to be a large source of OH radicals. VandenBoer et al. analyze these results in terms of rates for HONO production and loss and the integrated impact on both nitrogen oxides and OH.

[46] Wintertime measurements of OH radicals are relatively sparse compared to summertime, but they provide an important test of the understanding of radical production and propagation, since photolysis of nighttime radical reservoirs such as HONO and $ClNO_2$ may make a proportionally larger contribution to primary radicals. Kim et al. (submitted manuscript, 2013) report OH measurements near surface level (2 m) from NACHTT. They find surprisingly large OH concentrations, with an average midday (11 AM – 1 PM local) peak concentration of 2.7×10^6 molecules cm^{-3}. Although there is somewhat higher average UV actinic flux at the BAO site due to it higher elevation (~1600 m ASL) and generally clear weather, the contribution of ozone photolysis to primary OH production was estimated at only 15%. Photolysis of HONO, by contrast, contributed an estimated 80% of primary OH, while ozonolysis reactions of alkenes were responsible for an additional 5%. Due to lack of available measurements, other sources of HO_x, such as photolysis of formaldehyde, were not included in this budget, so the budget only compares the relative contribution of the sources listed above. This budget for primary OH production is unusual; other wintertime studies [*Heard et al*., 2004; *Ren et al*., 2006] have inferred large contributions of 36–57% from HONO photolysis, but also infer relatively larger inputs from alkene ozonolysis reactions. A base model that was unconstrained to HONO underestimated midday OH concentrations by more than a factor of 7, and morning OH by more than a factor of 20. Constraining the model to observed HONO reduced the model to measurement discrepancy to a factor of two at midday. The authors invoke strong vertical gradients in the local production of OH through the first few tens of meters above ground level to explain the remaining discrepancy. These results demonstrate the sensitivity of OH to heterogeneous processes and suggest that more research is required to understand radical production and its dependence on height during winter.

5.4. VOCs and Oil and Gas Emissions

[47] Measurements of VOCs proved to be a significant component of the NACHTT study. Originally included in order to understand air mass characteristics and origin, reactivities for radical species such as OH, Cl, and NO_3, and the degree of air mass processing or oxidation, the VOC measurements at NACHTT also demonstrated the influence of local emission from the oil and natural gas industry in the region. The BAO is located at the southwestern end of the Wattenberg field, an active oil and gas producing region within the Denver-Julesburg basin, with more than 14,000 active wells (see Figure 1).

[48] *Gilman et al.* [2013] reported a set of 53 speciated VOCs from near-surface measurements during NACHTT using an in situ GC-MS (Table 3). The most striking feature of these measurements was the large mixing ratios of light alkanes. The average level of propane, for example, was 27 ppbv, three to nine times larger than levels characteristic of other urban areas. Other VOCs, such as benzene and acetylene, did not show large enhancements relative to other urban measurements. The authors presented a methodology to distinguish the source of different VOCs based on their correlation with tracers for oil and gas emissions (propane) and urban emissions (acetylene). The analysis showed that 73–96% of the C_2–C_6 alkanes were attributable to emissions from oil and gas activities in the region. Furthermore, oil and gas emission were responsible for $55 \pm 18\%$ of the OH reactivity with VOCs, implicating these emissions as potentially important for ozone formation during summer. Although NACHTT was a wintertime campaign during which ozone was always less than the 75 ppbv 8 hour NAAQS, the results suggest that light alkane emissions could be an important contributor to ozone during summer months in Colorado's Front Range, currently designated as an ozone nonattainment area.

[49] Swarthout et al. (submitted manuscript, 2013) reported a set of 90 speciated VOCs from canister sampling at the fixed-height platform at 22 m, as well as vertical profiles from

canister samples at discrete heights on the tower. These measurements and their analysis were independent from those of *Gilman et al.* [2013], but reach similar conclusions regarding the influence of oil and gas emissions in the region. Swarthout et al. (submitted manuscript, 2013) found C_2–C_5 alkanes comprise 66% of the total VOCs (on a per molecule, rather than per carbon, basis), with a maximum summed mixing ratio of C_2–C_{10} alkanes reaching 336 ppbv. Their mean propane mixing ratio (16 ± 9 ppbv) was somewhat lower than *Gilman et al.* [2013], likely due to sampling at 22 m rather than 9 m above ground level. Mixing ratios of C_2–C_5 alkanes were an order of magnitude larger than winter mixing ratios reported at other suburban and rural sites. Similarly, mean propane from NACHTT was 10 times larger than the summertime average from 28 U.S. cities during summer 1999–2005 [*Baker et al.*, 2008], while mean ethene (0.43 ± 0.47 ppbv), an urban tracer, was about half of the mean urban values. Furthermore, alkane and alkyl nitrate (an oxidation product of alkanes) mixing ratios were significantly enhanced in north and northeast wind sectors (i.e., from the oil and gas area in Figure 1) while acetylene, aromatics, and oxygenated VOCs were more enhanced in southerly wind flow (from the urban area in Figure 1). These authors also demonstrated that the ratio of i-pentane to n-pentane of 1.0 was identical to that reported for raw natural gas and distinctly different than the ratio of 1.5 – 4 reported from other urban areas. Vertical profiles also showed increased mixing ratios of all VOCs near the surface, consistent with a local source. Thus, numerous source signatures implicated oil and natural gas activities in the enhanced light alkane mixing ratios. Swarthout et al. (submitted manuscript, 2013) also report dimethyl sulfide (DMS) mixing ratios varying over a range of several tens of parts per trillion and correlated with those of propane. They suggest DMS as a reduced sulfur component of natural gas emissions. Integrated yearly fluxes of different VOCs were estimated from the ambient measurements, suggesting for example an annual propane emission of 40 Gg. This flux is larger than that estimated from similar analyses in a gas-producing region of Oklahoma and Texas [*Katzenstein et al.*, 2003], but corroborates the range previously estimated for the Wattenberg field [*Pétron et al.*, 2012]. Finally, OH reactivity analysis showed alkanes to account for 49% of the total OH-VOC reactivity, well in excess of that observed in other areas, but similar to the conclusions of *Gilman et al.* [2013].

[50] Finally, the vertically resolved measurements during NACHTT included isocyanic acid, HNCO, a compound emitted during biomass burning and likely other combustion processes. J. M. Roberts et al. (New insights into atmospheric sources and sinks of isocyanic acid, HNCO, from recent urban and regional observations, submitted to *Journal of Geophysical Research,* 2013) (this issue) report these measurements together with comparisons to data from Pasadena, CA in spring-summer 2010 (CalNex) and Fort Collins, CO in summer 2011. Isocyanic acid during NACHTT has a larger background than during the two summertime data sets, indicating a regional source for this compound from wood burning during winter. During several instances, vertical profiles intercepted small agricultural fires that were rich in HNCO (up to 1.2 ppbv) as well as other species commonly emitted from fires (e.g., fine particles).

6. Conclusions

[51] NACHTT study was a three-week, wintertime field intensive in Colorado's Front Range urban corridor. It incorporated a series of both fixed-height and vertically resolved (0–270 m) measurements to characterize air pollutants and oxidant formation during the winter season. Major findings include the following.

[52] 1. Meteorology during NACHTT was characteristic of this region during winter and included upslope and downslope flows along the South Platte River valley that transported air pollutants across the region, as well as periods of strong downslope flow along the Rocky Mountain foothills that transported relatively cleaner air into the region.

[53] 2. Nitrate was the dominant component of aerosol mass, but there were also significant contributions from both organics and sulfate. Sulfate was associated primarily with long-range transport, while most of the nitrate was produced from precursors emitted within the region. OA could be subdivided into aged and primary components, with aged components more readily associated with sulfate and long-range transport, and primary or less aged components associated with nitrate, gas-phase nitrogen oxides, and shorter-range transport or local production.

[54] 3. Aerosol chloride, one of the key precursors for $ClNO_2$, was mainly present in the supermicron aerosol rather than submicron aerosol or gas-phase HCl. Total chloride mass was always in excess of gas-phase $ClNO_2$, indicating sufficient mass in the particulate phase to support gas-phase halogen activation through heterogeneous N_2O_5 uptake. The source of this chloride was not apparent, but its association with sodium suggests the long-range transport of marine aerosol from the Pacific, deflation of playa salts in the intermountain region to the west of Colorado, and/or local road salt.

[55] 4. Short-lived, gas-phase halocarbon compounds containing chlorine, bromine, and iodine, often used as tracers for marine air, appeared to have primarily local sources from industrial activity and/or water treatment in the area. There was little evidence for transport of marine-influenced air to the region based on these measurements.

[56] 5. Uptake coefficients for N_2O_5 varied from 0.002 to 0.1, but were sharply peaked between 0.01 and 0.02, a value larger than some recent summertime determinations. The presence of aerosol nitrate suppressed the N_2O_5 uptake, but not enough to make uptake rate limiting relative to the reaction of $NO_2 + O_3$ in determining overnight NO_x loss.

[57] 6. Nitryl chloride, $ClNO_2$, was highly variable. Its largest mixing ratios (up to 1.2 ppbv) occurred in plumes transported above surface level from the Denver urban area or from industrial or electric power generation point sources within this area. These plumes also contained aerosol chloride, suggesting a combustion source of both NO_x and soluble chloride, the ingredients for $ClNO_2$ production.

[58] 7. Nitrous acid varied strongly with height and was most clearly enhanced at low altitude (<50 m), indicating a source from NO_2 uptake to the ground surface. Surface deposition of HONO may have significantly limited the amount of HONO present in the gas phase. Nitrous acid was also present during daytime, when it served as a significant source of OH radicals at low altitude.

[59] 8. Near-surface (2 m) concentrations of OH radicals were surprisingly large for wintertime, with midday average peak levels of 2.7×10^6 molecules cm^{-3}. These levels

were far in excess of predictions from a box model. Inclusion of HONO improved the model to measurement agreement, but did not resolve it entirely without invoking stronger vertical gradients in HONO to the height of the OH measurement.

[60] 9. Large mixing ratios of light alkanes (e.g., average propane 27 ppbv near surface, 16 ppbv above the surface) were attributable to emissions from oil and gas activities, mainly to the north and east of the site. Light alkanes were responsible for up to 55% of the OH reactivity with VOCs, indicating that these VOC emissions are likely to be a contributing factor to ozone formation in this region during summertime.

[61] 10. Isocyanic acid, HNCO, a product of biomass burning and other combustion processes, had a larger background level in this winter study than in two recent summertime studies. The observations were consistent with emissions from residential wood burning and small agricultural fires in the area.

[62] **Acknowledgments.** This work was supported in part by NOAA's Atmospheric Chemistry and Climate Program. Financial support was also provided by the National Science Foundation through awards to the University of Virginia (ANT-1041187) and the University of New Hampshire (ANT-1041049) and Appalachian State University (ANT-1127774).

References

Anderson, J. A., D. L. Blumenthal, and G. J. Sen (1977), Characterization of Denver's urban plume using an instrumented aircraft, in *Denver Air Pollution Study - 1973*, edited by P. G. Russsell, pp. 3–34, U.S. Environ. Prot. Agency, Denver, Colo.

Bahreini, R., E. J. Dunlea, B. M. Matthew, C. Simons, K. S. Docherty, P. F. DeCarlo, J. L. Jimenez, C. A. Brock, and A. M. Middlebrook (2008), Design and operation of a pressure-controlled inlet for airborne sampling with an aerodynamic aerosol lens, *Aerosol Sci. Technol.*, *42*(6), 465–471, doi:10.1080/02786820802178514.

Bahreini, R., et al. (2009), Organic aerosol formation in urban and industrial plumes near Houston and Dallas, Texas, *J. Geophys. Res.*, *114*, D00F16, doi:10.1029/2008JD011493.

Baker, A. K., A. J. Beyersdorf, L. A. Doezema, A. S. Katzenstein, S. Meinardi, I. J. Simpson, D. R. Blake, and F. S. Rowland (2008), Measurements of nonmethane hydrocarbons in 28 United States cities, *Atmos. Environ.*, *42*, 170–182.

Baker, K. R., H. Simon, and J. T. Kelly (2011), Challenges to modeling cold pool meteorology associated with high pollution episodes, *Environ. Sci. Technol.*, *45*(17), 7118–7119, doi:10.1021/es202705v.

Benedict, K. B., D. Day, F. M. Schwandner, S. M. Kreidenweis, B. Schichtel, W. C. Malm, and J. L. Collett Jr. (2013), Observations of atmospheric reactive nitrogen species in Rocky Mountain National Park and across northern Colorado, *Atmos. Environ.*, *64*(0), 66–76, doi:10.1016/j.atmosenv.2012.08.066.

Bertram, T. H., J. A. Thornton, T. P. Riedel, A. M. Middlebrook, R. Bahreini, T. S. Bates, P. K. Quinn, and D. J. Coffman (2009), Direct observations of N_2O_5 reactivity on ambient aerosol particles, *Geophys. Res. Lett.*, *36*, L19803, doi:10.1029/2009GL040248.

Blanken, P. D., J. Dillon, and G. Wismann (2001), The impact of an air quality advisory program on voluntary mobile source air pollution reduction, *Atmos. Environ.*, *35*(13), 2417–2421.

Brock, C. A., et al. (2011), Characteristics, sources, and transport of aerosols measured in spring 2008 during the aerosol, radiation, and cloud processes affecting Arctic Climate (ARCPAC) Project, *Atmos. Chem. Phys.*, *11*(6), 2423–2453, doi:10.5194/acp-11-2423-2011.

Brodin, M., D. Helmig, and S. Oltmans (2010), Seasonal ozone behavior along an elevation gradient in the Colorado Front Range Mountains, *Atmos. Environ.*, *44*(39), 5305–5315.

Brown, S. S., et al. (2006a), Nocturnal odd-oxygen budget and its implications for ozone loss in the lower troposphere, *Geophys. Res. Lett.*, *33*, L08801, doi:10.1029/2006GL025900.

Brown, S. S., et al. (2006b), Variability in nocturnal nitrogen oxide processing and its role in regional air quality, *Science*, *311*, 67–70.

Brown, S. S., W. P. Dubé, H. D. Osthoff, D. E. Wolfe, W. M. Angevine, and A. R. Ravishankara (2007), High resolution vertical distributions of NO_3 and N_2O_5 through the nocturnal boundary layer, *Atmos. Chem. Phys.*, *7*, 139–149.

Brown, S. S., et al. (2009), Reactive uptake coefficients for N_2O_5 determined from aircraft measurements during TexAQS 2006: Comparison to current model parameterizations, *J. Geophys. Res.*, *114*, D00F10, doi:10.1029/2008JD011679.

Burns, S., S. J. Frey, J. C. Chow, J. G. Watson, and C. S. Sloane (1990), An overview of the 1987-88 Metro Denver Brown Cloud Study, in *Visibility and Fine Particles*, edited by C. V. Mathai, pp. 363–373, Air and Waste Manage. Assoc., Pittsburgh, Pa.

Cai, C., C. Hogrefe, P. Katsafados, G. Kallos, M. Beauharnois, J. J. Schwab, X. Ren, W. H. Brune, X. Zhou, Y. He, and K. L. Demerjian (2008), Performance evaluation of an air quality forecast modeling system for a summer and winter season—Photochemical oxidants and their precursosrs, *Atmos. Environ.*, *42*, 8585–8599.

Carter, W. P. L., and J. H. Seinfeld (2012), Winter ozone formation and VOC incremental reactivities in the Upper Green River Basin of Wyoming, *Atmos. Environ.*, *50*(0), 255–266, doi:10.1016/j.atmosenv.2011.12.025.

Chang, W. L., P. V. Bhave, S. S. Brown, N. Riemer, J. Stutz, and D. Dabdub (2011), Heterogeneous atmospheric chemistry, ambient measurements, and model calculations of N_2O_5: A review, *Aerosol Sci. Technol.*, *45*, 655–685.

Chen, J., Q. Ying, and M. J. Kleeman (2010), Source apportionment of wintertime secondary organic aerosol during the California regional PM10/PM2.5 air quality study, *Atmos. Environ.*, *44*(10), 1331–1340.

Chen, L. W. A., J. G. Watson, J. C. Chow, M. C. Green, D. Inouye, and K. Dick (2012), Wintertime particulate pollution episodes in an urban valley of the Western US: A case study, *Atmos. Chem. Phys.*, *12*(21), 10,051–10,064, doi:10.5194/acp-12-10,051-10,064.

Countess, R. J., G. T. Wolff, and S. H. Cadle (1980), The Denver winter aerosol: A comprehensive chemical characterization, *J. Air Pollut. Control Assoc.*, *30*(11), 1194–1200.

Countess, R. J., S. H. Cadle, P. J. Groblicki, and G. T. Wolff (1981), Chemical analysis of size-segregated samples of Denver's ambient particulate, *J. Air Pollut. Control Assoc.*, *31*(3), 247–252.

Crow, L. W. (1977), Airflow study related to EPA field monitoring program Denver metropolitan area November, 1973, in *Denver Air Pollution Study - 1973*, edited by P. G. Russsell, pp. 3–30, U.S. Environ. Prot. Agency, Denver, Colo.

Dentener, F. J., and P. J. Crutzen (1993), Reaction of N_2O_5 on tropospheric aerosols: Impact on the global distributions of NO_x, O_3, and OH, *J. Geophys. Res.*, *98*(D4), 7149–7163.

Dietrich, D. L., J. V. Molnar, J. F. Faust, and J. G. Watson (1990), Transmissometer extinction measurements in an urban environment, in *Visibility and Fine Particles*, edited by C. V. Mathai, pp. 374–383, Air and Waste Manage. Assoc., Pittsburg, Pa.

Dutton, S. J., B. Rajagopalan, S. Vedal, and M. P. Hannigan (2010), Temporal patterns in daily measuremetns of inorganic and organic speciated PM2.5 in Denver, *Atmos. Environ.*, *44*, 987–998.

Ferman, M. A., G. T. Wolff, and N. A. Kelly (1981), An assessment of the gaseous-pollutants and meteorological conditions associated with Denver Brown Cloud, *J. Environ. Sci. Health, Part A Environ. Sci. Eng. Toxic Hazard. Subst. Control*, *16*(3), 315–339.

Finlayson-Pitts, B. J., M. J. Ezell, and J. N. J. Pitts (1989), Formation of chemically active chlorine compounds by reactions of atmospheric NaCl particles with gaseous N_2O_5 and $ClONO_2$, *Nature*, *337*, 241–244.

Finlayson-Pitts, B. J., L. M. Wingen, A. L. Sumner, D. Syomin, and K. A. Ramazan (2003), The heterogeneous hydrolysis of NO_2 in laboratory systems and in outdoor and indoor atmospheres: An integrated mechanism, *Phys. Chem. Chem. Phys.*, *5*(2), 223–242.

Fischer, E., and R. Talbot (2005), Regional NO_3^- events in the northeastern United State related to seasonal climate anomalies, *Geophys. Res. Lett.*, *32*, L16804, doi:10.1029/2005GL023490.

Fleming, Z. L., P. S. Monks, A. R. Rickard, B. J. Bandy, N. Brough, T. J. Green, C. E. Reeves, and S. A. Penkett (2006), Seasonal dependence of peroxy radical concentrations at a northerm hemisphere marine boundary layer site during summer and winter: Evidence for photochemical activity in winter, *Atmos. Chem. Phys.*, *6*, 5415–5433.

Fuchs, H., W. P. Dubé, B. M. Lerner, N. L. Wagner, E. J. Williams, and S. S. Brown (2009), A sensitive and versatile detector for atmospheric NO_2 and NO_x based on blue diode laser cavity ring-down spectroscopy, *Environ. Sci. Technol.*, *43*, 7831–7836.

Gilman, J. B., et al. (2009), Measurements of volatile organic compounds during the 2006 TexAQS/GoMACCS campaign: Industrial influences, regional characteristics, and diurnal dependencies of the OH reactivity, *J. Geophys. Res.*, *114*, D00F06, doi:10.1029/2008JD011525.

Gilman, J. B., B. M. Lerner, W. C. Kuster, and J. A. de Gouw (2013), Source signature of volatile organic compounds from oil and natural gas operations in northeastern Colorado, *Environ. Sci. Technol.*, *47*(3), 1297–1305, 10.1021/es304119a.

Groblicki, P. J., G. T. Wolff, and R. J. Countess (1981), Visibility-reducing species in the Denver Brown Cloud. 1. Relationships between extinction and chemical-composition, *Atmos. Environ.*, *15*(12), 2473–2484.

Haagenson, P. L. (1979), Meteorological and climatological factors affecting Denver air-quality, *Atmos. Environ.*, *13*(1), 79–85.

Hahn, C. J. (1981), A study of the diurnal behavior of boundary-layer winds at the Boulder Atmospheric Observatory, *Boundary Layer Meteorol.*, *21*(2), 231–245.

Heard, D. E., L. J. Carpenter, D. J. Creasey, J. R. Hopkins, J. D. Lee, A. C. Lewis, M. J. Pilling, and P. W. Seakins (2004), High levels of the hydroxyl radical in the winter urban troposphere, *Geophys. Res. Lett.*, *31*, L18112, doi:10.1029/2004GL020544.

Houck, J. E., J. M. Goulet, J. C. Chow, J. G. Watson, and L. C. Pritchett (1990), Chemical characterization of emission sources contributing to light extinction, in *Visibility and Fine Particles*, edited by C. V. Mathai, pp. 437–446, Air and Waste Manage. Assoc., Pittsburgh, Pa.

Kaimal, J. C., and J. E. Gaynor (1983), The Boulder Atmospheric Observatory, *J. Clim. Appl. Meteorol.*, *22*(5), 863–880.

Katzenstein, A. S., L. A. Doezema, I. J. Simpson, D. R. Blake, and F. S. Rowland (2003), Extensive regional atmospheric hydrocarbon pollution in the southwestern United States, *Proc. Natl. Acad. Sci. U. S. A.*, *100*(21), 11,975–11,979.

Katzman, T. L., A. P. Rutter, J. J. Schauer, G. C. Lough, C. J. Kolb, and S. Van Klooster (2010), PM2.5 and PM10-2.5 compositions during wintertime episodes of elevated PM concentrations across the midwestern USA, *Aerosol Air Qual. Res.*, *10*, 140–153.

Keene, W. C., M. S. Long, A. A. P. Pszenny, R. Sander, J. R. Maben, A. J. Wall, T. L. O'Halloran, A. Kerkweg, E. V. Fischer, and O. Schrems (2009), Latitudinal variation in the multiphase chemical processing of inorganic halogens and related species over the eastern North and South Atlantic Oceans, *Atmos. Chem. Phys.*, *9*(19), 7361–7385.

Kercher, J. P., T. P. Riedel, and J. A. Thornton (2009), Chlorine activation by N_2O_5: simultaneous, in-situ detection of $ClNO_2$ and N_2O_5 by chemical ionization mass spectrometry, *Atmos. Meas. Tech.*, *2*, 193–204.

Kleffmann, J., R. Kurtenbach, J. Lörzer, P. Wiesen, N. Kalthoff, B. Vogel, and H. Vogel (2003), Measured and simulated vertical profiles of nitrous acid—Part I: Field measurements, *Atmos. Environ.*, *37*, 2949–2955.

Klinedinst, D. B., and L. A. Currie (1999), Direct quantification of PM2.5 fossil and biomass carbon within the Northern Front Range Air Quality Study's domain, *Environ. Sci. Technol.*, *33*(23), 4146–4154.

Koken, P. J. M., W. T. Piver, F. Ye, A. Elixhauser, L. M. Olsen, and C. J. Portier (2003), Temperature, air pollution, and hospitalization for cardiovascular diseases among elderly people in Denver, *Environ. Health Perspect.*, *111*(10), 1312–1317.

Lawler, M. J., B. D. Finley, W. C. Keene, A. A. P. Pszenny, K. A. Read, R. von Glasow, and E. S. Saltzman (2009), Pollution-enhanced reactive chlorine chemistry in the eastern tropical Atlantic boundary layer, *Geophys. Res. Lett.*, *36*, L08810, doi:10.1029/2008GL036666.

Levin, E. J. T., S. M. Kreidenwies, G. R. McMeeking, C. M. Carrico, J. L. Collett, and W. C. Malm (2009), Aerosol physical, chemical and optical properties during the Rocky Mountain Airborne Nitrogen and Sulfur study, *Atmos. Environ.*, *43*, 1932–1939.

Levy, H. (1971), Normal atmosphere: Large radical and formaldehyde concentrations predicted, *Science*, *173*, 141–143.

Lewis, C. W., R. H. Baumgardner, R. K. Stevens, and G. M. Russwurm (1986), Receptor modeling study of Denver winter haze, *Environ. Sci. Technol.*, *20*(11), 1126–1136.

Mathur, R., S. Yu, D. Kang, and K. L. Schere (2008), Assessment of the wintertime performance of developmental particulate matter forecasts with the Eta-Community Multiscale Air Quality modeling system, *J. Geophys. Res.*, *113*, D02303, doi:10.1029/2007JD008580.

McCulloch, A., M. L. Aucott, C. M. Benkovitz, T. E. Graedel, G. Kleiman, P. M. Midgley, and Y.-F. Li (1999), Global emissions of hydrogen chloride and chloromethane from coal combustion, incineration and industrial activities: Reactive chlorine emissions inventory, *J. Geophys. Res.*, *104*(D7), 8931–8403, doi:10.1029/1999JD900025.

Mielke, L. H., A. Furgeson, and H. D. Osthoff (2011), Observation of $ClNO_2$ in a mid-continental urban environment, *Environ. Sci. Technol.*, *45*(20), 8889–8896, 10.1021/es201955u.

Moosmuller, H., W. P. Arnott, C. F. Rogers, J. C. Chow, C. A. Frazier, L. E. Sherman, and D. L. Dietrich (1998), Photoacoustic and filter measurements related to aerosol light absorption during the Northern Front Range Air Quality Study (Colorado 1996/1997), *J. Geophys. Res.*, *103*(D21), 28,149–28,157.

Nanus, L., D. H. Campbell, G. P. Ingersoll, D. W. Clow, and M. A. Mast (2003), Atmospheric deposition maps for the Rocky Mountains, *Atmos. Environ.*, *37*(35), 4881–4892.

Neff, W. D. (1997), The Denver Brown Cloud studies from the perspective of model assessment needs and the role of meteorology, *J. Air Waste Manage. Assoc.*, *47*(3), 269–285.

Neff, W. D., and J. G. Watson (1990), Evaluation of the fuel-switching strategy used on the Denver Brown Cloud Study, in *Visibility and Fine Particles*, edited by C. V. Mathai, pp. 410–421, Air and Waste Manage. Assoc., Pittsburgh, Pa.

Osthoff, H. D., et al. (2008), High levels of nitryl chloride in the polluted subtropical marine boundary layer, *Nat. Geosci.*, *1*, 324–328.

Perner, D., and U. Platt (1979), Detection of nitrous acid in the atmosphere by differential optical absorption spectroscopy, *Geophys. Res. Lett.*, *6*(2), 971–920.

Pétron, G., et al. (2012), Hydrocarbon emissions characterization in the Colorado Front Range: A pilot study, *J. Geophys. Res.*, *117*, D04304, 10.1029/2011JD016360.

Phillips, G. J., M. J. Tang, J. Thieser, B. Brickwedde, G. Schuster, B. Bohn, J. Lelieveld, and J. N. Crowley (2012), Significant concentrations of nitryl chloride observed in rural continental Europe associated with the influence of sea salt chloride and anthropogenic emissions, *Geophys. Res. Lett.*, *39*, L10811, doi:10.1029/2012GL051912.

Prospero, J. M., M. Uematsu, and D. L. Savoie (1989), Mineral aerosol transport to the Pacific Ocean, in *SEAREX: The Sea-Air Exchange Program, Chemical Oceanography*, Volume 10, pp. 187–218, edited by Riley, J. P., R. Chester, and R. A. Duce, Academic Press, London.

Reddy, P. J., D. E. Barbarick, and R. D. Osterburg (1995), Development of a statistical-model for forecasting episodes of visibility degradation in the Denver Metropolitan-Area, *J. Appl. Meteorol.*, *34*(3), 616–625.

Ren, X., et al. (2006), Behavior of OH and HO_2 in the winter atmosphere in New York City, *Atmos. Environ.*, *40*, suppl. 2, S252–S263.

Richards, L. W., C. S. Sloane, J. G. Watson, and J. C. Chow (1990), Exticntion apportionment for the Denver Brown Cloud, in *Visibility and Fine Particles*, edited by C. V. Mathai, pp. 394–409, Air and Waste Manage. Assoc., Pittsburg, Pa.

Riedel, T. P., et al. (2012a), Nitryl chloride and molecular chlorine in the coastal marine boundary layer, *Environ. Sci. Technol.*, *46*, 10,463–10,470, doi:dx.doi.org/10.1021/es204632r.

Riedel, T. P., T. H. Bertram, O. S. Ryder, S. Liu, D. A. Day, L. M. Russell, C. J. Gaston, K. A. Prather, and J. A. Thornton (2012b), Direct N_2O_5 reactivity measurements at a polluted coastal site, *Atmos. Chem. Phys.*, *12*(6), 2959–2968, doi:10.5194/acp-12-2959-2012.

Riehl, H., and D. Herkhof (1972), Some aspects of Denver air pollution meteorology, *J. Appl. Meteorol.*, *11*, 1040–1047.

Riemer, N., H. Vogel, B. Vogel, B. Schell, I. Ackerman, C. Kessler, and H. Hass (2003), Impact of the heterogeneous hydrolysis of N_2O_5 on chemistry and nitrate aerosol formation in the lower troposphere under photosmog conditions, *J. Geophys. Res.*, *108*(D4), 4144, doi:10.1029/2002JD002436.

Roberts, J. M., et al. (2010), Measurement of HONO, HNCO, and other inorganic acids by negative-ion proton-transfer chemical-ionization mass spectrometry (NI-PT-CIMS): Application to biomass burning emissions, *Atmos. Meas. Tech.*, *3*, 981–990.

Russell, P. A. (1977), *Denver Air Pollution Study - 1973*, U.S. Environ. Prot. Agency, Denver, Colo.

Russell, K. M., W. C. Keene, J. R. Maben, J. N. Galloway, and J. L. Moody (2003), Phase-partitioning and dry deposisition of atmospheric nitrogen at the mid-Atlantic U.S. Coast, *J. Geophys. Res.*, *108*(D21), 4656, doi:10.1029/2003JD003736.

Russo, R. S., Y. Zhou, K. B. Haase, O. W. Wingenter, E. K. Frinak, H. Mao, R. W. Talbot, and B. C. Sive (2010), Temporal variability, sources, and sinks of C1 - C5 alklyl nitrates in coastal New England, *Atmos. Chem. Phys.*, *10*(4), 1865–1883.

Schaap, M., M. van Loon, H. M. ten Brink, F. J. Dentener, and P. J. H. Builtjes (2004), Secondary inorganic aerosol simulations for Europe with special attention to nitrate, *Atmos. Chem. Phys.*, *4*(3), 857–874.

Schnell, R. C., S. J. Oltmans, R. R. Neely, M. S. Endres, J. V. Molenar, and A. B. White (2009), Rapid photochemical production of ozone at high concentrations in a rural site during winter, *Nat. Geosci.*, *2*, 120–122.

Silkoff, P. E., L. N. Zhang, S. Dutton, E. L. Langmack, S. Vedal, J. Murphy, and B. Make (2005), Winter air pollution and disease parameters in advanced chronic obstructive pulmonary disease panels residing in Denver, Colorado, *J. Allergy Clin. Immunol.*, *115*(2), 337–344.

Sive, B. C., Y. Zhou, D. Troop, Y. Wang, W. C. Little, O. W. Wingenter, R. S. Russo, R. h. K. Varner, and R. Talbot (2005), Development of a cryogen-free concentration system for measurements of volatile organic compounds, *Anal. Chem.*, *77*(21), 6989–6998, doi:10.1021/ac0506231.

Sloane, C. S., J. G. Watson, J. C. Chow, L. Pritchett, and L. W. Richards (1990), Size distribution and optical properties of the Denver Brown Cloud, in *Visibility and Fine Particles*, edited by C. V. Mathai, pp. 384–393, Air and Waste Manage. Assoc., Pittsburgh, Pa.

Sloane, C. S., J. Watson, J. Chow, L. Pritchett, and L. W. Richards (1991), Size-segregated fine particle measurements by chemical-species and their impact on visibility impairment in Denver, *Atmos. Environ. Part A*, *25*(5-6), 1013–1024.

Stanier, C., et al. (2012), Overview of the LADCO winter nitrate study: Hourly ammonia, nitric acid and PM2.5 composition at an urban and rural site pair during PM2.5 episodes in the US Great Lakes region, *Atmos. Chem. Phys.*, *12*(22), 11,037–11,056, doi:10.5194/acp-12-11037-2012.

Stark, H., B. M. Lerner, R. Schmitt, R. Jakoubek, E. J. Williams, T. B. Ryerson, D. T. Sueper, D. D. Parrish, and F. C. Fehsenfeld (2007), Atmospheric in situ measurement of nitrate radical (NO3) and other photolysis rates using spectroradiometry and filter radiometry, *J. Geophys. Res.*, *112*, D10S04, doi:10.1029/2006JD007578.

Stemmler, K., M. Ammann, C. Donders, J. Kleffmann, and C. George (2006), Photosensitized reduction of nitrogen dioxide on humic acid as a source of nitrous acid, *Nature*, *440*, 195–198.

Stutz, J., B. Alicke, and A. Neftel (2002), Nitrous acid formation in the urban atmosphere: Gradient measurements of NO_2 and HONO over grass in Milan, Italy, *J. Geophys. Res.*, *107*(D22), 8192, doi:10.1029/2001JD000390.

Stutz, J., H.-J. Oh, S. I. Whitlow, C. Anderson, J. E. Dibb, J. H. Flynn, B. Rappenglück, and B. Lefer (2010), Simultaneous DOAS and mist-chamber IC measurements of HONO in Houston, TX, *Atmos. Environ.*, *44*(33), 4090–4098.

Su, H., Y. F. Cheng, M. Shao, D. F. Gao, Z. Y. Yu, L. M. Zeng, J. Slanina, Y. H. Zhang, and A. Wiedensohler (2008), Nitrous acid (HONO) and its daytime sources at a rurual site during the 2004 PRIDE-PRD experiment in China, *J. Geophys. Res.*, *113*, D14312, doi:10.1029/2007JD009060.

Tanner, D. J., A. Jefferson, and F. L. Eisele (1997), Selected ion chemical ionization mass spectrometric measurement of OH, *J. Geophys. Res.*, *102*(D5), 6415–6425.

Thornton, J. A., et al. (2010), A large atomic chlorine source inferred from mid-continental reactive nitrogen chemistry, *Nature*, *464*, 271–274.

Tolocka, M. P., P. A. Solomon, W. Mitchell, G. A. Norris, D. B. Gemmill, R. W. Wiener, R. W. Vanderpool, J. B. Homolya, and J. Rice (2001), East versus West in the US: Chemical characteristics of PM2.5 during the winter of 1999, *Aerosol Sci. Technol.*, *34*, 88–96.

Toth, J. J., and R. H. Johnson (1985), Summer surface flow characteristics over northeast Colorado, *Mon. Weather Rev.*, *113*(9), 1458–1469.

Vanvalin, C. C., and E. Ganor (1987), Air-pollution measurements at the Boulder-Atmospheric-Observatory, *Water Air Soil Pollut.*, *35*(3-4), 357–372.

Veres, P., J. M. Roberts, C. Warneke, D. Welsh-Bon, M. Zahniser, S. Herndon, R. Fall, and J. de Gouw (2008), Development of negative-ion proton-transfer chemical-ionization mass spectrometry (NI-PT-CIMS) for the measurement of gas-phase organic acids in the atmosphere, *Int. J. Mass Spectrom.*, *274*, 48–55.

Waggoner, A. P. (1977), The Brown Cloud of Denver, in *Denver Air Pollution Study - 1973*, edited by P. G. Russell, pp. 159–167, U.S. Environ. Prot. Agency, Denver, Colo.

Wagner, N. L., W. P. Dubé, R. A. Washenfelder, C. J. Young, I. B. Pollack, T. B. Ryerson, and S. S. Brown (2011), Diode laser-based cavity ring-down instrument for NO_3, N_2O_5, NO, NO_2 and O_3 from aircraft, *Atmos. Meas. Tech.*, *4*, 1227–1240.

Wagner, N. L., et al. (2012), The sea breeze / land breeze circulation in Los Angeles and its influence on nitryl chloride production and air quality in this region, *J. Geophys. Res.*, *116*, D00V24, doi:10.1029/2012JD017810.

Washenfelder, R. A., W. P. Dubé, N. L. Wagner, and S. S. Brown (2011), Measurement of atmospheric ozone by cavity ring-down spectroscopy, *Environ. Sci. Technol.*, *45*, 2938–2944.

Watson, J. G., J. C. Chow, L. C. Pritchett, J. A. Houck, S. Burns, and R. A. Ragazzi (1990), Composite source profiles for particulate motor vehicle exhaust source apportionment in Denver, CO., in *Visibility and Fine Particles*, edited by C. V. Mathai, pp. 422–436, Air and Waste Manage. Assoc., Pittsburgh, Pa.

Watson, J. G., E. M. Fujita, J. C. Chow, B. Zielinska, L. W. Richards, W. Neff, and D. L. Dietrich (1998), Northern Front Range Air Quality Study final report, Desert Res. Inst., LOCATION.

Williams, E. J., F. C. Fehsenfeld, B. T. Jobson, W. C. Kuster, P. D. Goldan, J. Stutz, and W. A. McClenny (2006), Comparison of ultraviolet absorbance, chemiluminescence, and DOAS instruments for ambient ozone monitoring, *Environ. Sci. Technol.*, *40*, 5755–5762.

Wolff, G. T., R. J. Countess, P. J. Groblicki, M. A. Ferman, S. H. Cadle, and J. L. Muhlbaier (1981), Visibility-reducing species in the Denver Brown Cloud. 2. Sources and temporal patterns, *Atmos. Environ.*, *15*(12), 2485–2502.

Young, C. J., et al. (2012), Vertically resolved measurements of nighttime radical reservoirs in Los Angeles and their contribution to the urban radical budget, *Environ. Sci. Technol.*, *46*, 10,965–10,973, 10.1021/es302206a.

Yu, S., R. Dennis, S. Roselle, A. Nenes, J. Walker, B. Eder, K. Schere, J. Swall, and W. Robarge (2005), An assessment of the ability of three-dimensional air quality models with current thermodynamic equilibrium models to predict aerosol NO_3, *J. Geophys. Res.*, *110*, D07S13, doi:10.1029/2004JD004718.

Zhang, N., X. Zhou, P. B. Shepson, H. Gao, M. Alaghmand, and B. Stirm (2009), Aircraft measurement of HONO vertical profiles over a forested region, *Geophys. Res. Lett.*, *36*, L15820, doi:10.1029/2009GL038999.

Zhou, Y., H. Mao, R. S. Russo, D. R. Blake, O. W. Wingenter, K. B. Haase, J. Ambrose, R. K. Varner, R. Talbot, and B. C. Sive (2008), Bromoform and dibromomethane measurements in the seacoast region of New Hampshire, 2002–2004, *J. Geophys. Res.*, *113*, D08305, doi:10.1029/2007JD009103.